Free Actin and Effects on Lung Macrophage Bacterial Defenses

Free Actin and Effects on Lung Macrophage Bacterial Defenses

A dissertation presented
by

Christine Marie Ordija

to

Biological Sciences in Public Health

in partial fulfillment of the requirements

for the degree of

Doctor of Philosophy

in the subject of

Biological Sciences in Public Health

Harvard University

Cambridge, Massachusetts

January 2017

Christine Marie Ordija

Free Actin and Effects on Lung Macrophage Bacterial Defenses

Dissertation Advisor: Professor Lester Kobzik

Actin release into the circulation and extracellular space, with subsequent removal by the actin scavenging protein plasma gelsolin (pGSN), has long been reported in injury and infection. Our laboratory's recent finding that pGSN improved survival in a murine primary pneumococcal pneumonia model via macrophage nitric oxide synthase type III (NOS3) enhancement underscored pGSN's therapeutic potential, but also suggested the possibility of a more significant role for exposed actin in lung macrophage host defenses. Inflamed and injured lungs are more prone to bacterial infection, yet the ability of extracellular actin released from damaged tissue and cells to depress host defense has not been studied. In patients following burn and inhalation injury, and in murine models of oxidizing injury, influenza, and postinfluenza secondary pneumococcal pneumonia, we detected free actin release into the lung alveolar fluid via Western Blotting. We further demonstrate that free actin impairs alveolar macrophage binding and uptake of bacteria by interfering with the function of the scavenger receptor MARCO. In CFU bacterial binding assays in vitro, a murine alveolar macrophage cell line exhibited reduced binding and uptake of *Streptococcus pneumoniae*, *Staphylococcus aureus* and *Escherichia coli* in the presence of free actin. Similarly, primary human alveolar macrophage host defenses were impaired in the presence of actin, as observed via reduced binding and uptake of fluorescent-*S. aureus* in assays analyzed using scanning cytometry. Bacterial binding and uptake were restored through addition of pGSN, a highly conserved member of the extracellular

actin scavenging system (EASS). We then demonstrated a mechanism of free actin interaction with macrophages. A647-tagged fluorescent actin bound a murine lung macrophage derived cell line and primary human alveolar macrophages as observed via flow cytometry. Actin binding by AMs was reduced under pan-scavenger receptor inhibitors and in a MARCO / SRAI/II DKO cell line, pointing to scavenger receptor mediated actin binding. Ex vivo pan-scavenger receptor treated AMs obtained from MARCO -/- mice via bronchoalveolar lavage (BAL) exhibited even greater reductions in actin binding under flow cytometry, furthering implicating the MARCO receptor as an actin-binding AM partner. Free actin impairment of macrophage host defenses following release during injury and infection may be widespread and thus clinically relevant, further underscoring the importance of characterizing actin-macrophage interactions and the potential value of pGSN as a therapeutic immunomodulator.

Table of Contents

Dedication

To my parents with love, I certainly wouldn't be here without you.

Figure List

Chapter

Chapter 2

Appendix

Thesis Introduction

Actin has long been known as a component of the cytoskeleton and major constituent of muscle. More recently, new roles for actin in times of cellular stress and injury have been discovered. For example, free actin release from necrotic cells into the circulation or extracellular space occurs in a number of disease and inflammatory states (1-4). Our laboratory recently found that the actin-scavenging protein plasma gelsolin (pGSN) enhances macrophage nitric oxide (NO) synthase type III (NOS3) to improve survival in a murine model of primary and postinfluenza secondary pneumonia (5). This led us to wonder if free actin could also play a role in impairment of host defense. Inflamed and injured lungs are more prone to bacterial infection (6-9), thus we sought to first demonstrate the presence of free actin in a variety of injured or infected lungs. As lung macrophages provide the first line of host defense against invaders, we next assessed any effects of free actin on macrophage binding and uptake of bacteria, with a final focus on a mechanism by which actin may interfere with normal macrophage function, through interaction with the scavenger receptor MARCO.

Basic Actin Biochemistry and Function

Actin is a ubiquitous, multifunctional and highly conserved protein found in nearly all eukaryotic cells. Critical to the cytoskeleton and the contractile unit in muscle cells, actin is involved in a myriad of cell processes including movement, cell structure, development (10), gene transcription, chromosome morphology (11), DNA repair (12-16), and cell cycle control (17), among others. It is incredibly abundant, comprising 10% or more of total cellular protein, and has a great tendency to form filaments. With a mass of roughly 42 kDa, the actin polypeptide

is quite flat with 375 residues, 4 subdomains and two binding clefts, one for ATP or ADP and the other for several different actin-binding proteins (18). Monomers of globular (G) actin assemble to form filamentous (F) actin with the aid of regulatory actin binding proteins inside cells. Two strands of subunits arranged in right-hand helices comprise actin filaments, sometimes described as a single-left handed helix. Intracellular actin filaments become cross-linked and associated with cell membranes (19). Actin filaments have a polarity, characterized by 'barbed' and 'pointed' ends, as monomers associate and dissociate at different rate constants from each end (18). At least six different actin isoforms or isoactins have been identified in mammals, each encoded by a single gene and distinguished by a unique amino-terminal tryptic peptide (20). The isoactin multigene family encodes: α-skeletal muscle, α-cardiac muscle, α-smooth muscle, β-cytoplasmic, γ-cytoplasmic and γ-smooth muscle actins (21). Isoactins exhibit both differences and overlap in their function and tissue distribution. γ-cytoplasmic actin is high during and after development in the lung for example (10). Despite similarities in overall structure, polymerization properties between isoactins can differ (22) and these differences may extend to actin binding protein interactions.

Actin Presence in Lung and Tissue Injury

Actin may be functional and benign when contained within cells and muscle, yet it can play varied roles in disease progression and its release is observed in multiple infection and injury states. Elevated actin levels have been detected in burn wound fluid (23) and the postshock mesenteric lymph (PSML) of an experimental rodent model (24) and in that of trauma patients (25). It has been detected in the plasma of a hemorrhagic rodent model (26) and that of patients with septic shock (27), hepatic necrosis (28, 29), some complicated pregnancies (30), severe

Plasmodium falciparum malaria (31), and acute respiratory distress syndrome (ARDS) (4, 32). Actin γ 1 (ACTG1) was monitored in the BALF during ARDS and clearly observed to rise and fall over the course of the disease (1). Proteomic and gene ontology (GO) enrichment analysis of BALF from ARDS *non-survivors* showed elevated levels of proteins involved in actin cytoskeleton reorganization associated with cellular damage. Although unclear if associated with intracellular *and/or* free, extracellular actin, the G actin-sequestration protein Thymosin-like 2 (TMSB4X), the actin-binding and polymerization regulator Profilin 1 (PFN1), the F and G-actin binding protein Vasodilator-stimulated phosphoprotein (VASP), and Filamin A alpha (FLNA), a protein crosslinking actin filaments to membrane glycoproteins, were all elevated in ARDS (1, 33). Similarly, proteomic analysis of bronchoalveolar lavage fluid (BALF) from patients with ventilator-associated pneumonia (VAP), a frequent and dangerous complication of acute lung injury (ALI), shows elevated levels of an actin crosslinking protein, actinin 1 (ACTN1) (34).

Extracellular exposed actin may serve as a biomarker of tissue injury itself. The exact state and degree of free actin exposure may vary, namely as aggregated filaments attached to the membranes of ruptured cells, as exposed filaments on microparticles released by dying cells or even as G actin monomers. The body has notably created antibodies to actin in several states of disease and stress. Auto-antibodies to skeletal muscle actin are elevated in the circulation of trauma patients (35). After cardiac surgery, myocardial infarction (36) and in patients with autoimmune hepatitis, circulating autoantibodies to actin are again present (37). Importantly, actin filaments exposed on necrotic cells have been identified as Damage-Associated Molecular Patterns (DAMPs), one of several highly conserved evolutionary markers involved in tissue injury recognition and the initiation of sterile inflammation. Actin filaments are also now known

ligands for the C-type lectin receptor Clec9a (DNGR-1) (38-40), a dendritic cell receptor that recognizes necrotic cells (41). Further characterization of the progression of actin exposure or release, the cells and receptors types with which free actin interacts and the pattern of resultant cytokines generated, is likely to elucidate a highly conserved role for actin in the non-infectious inflammatory state.

Free Actin May be Harmful

Free actin release may be damaging due to fluid mechanics obstruction, complicated biochemical effects and additional, currently unknown mechanisms (2). At plasma salt concentrations, globular (G-actin) monomers are believed to polymerize to form double-helical filaments of F-actin upon release from necrotic cells into the circulation or extracellular fluid (3, 4). Intravenous injection of high concentrations of G-actin monomers is fatal in rats for example, with intravascular actin filaments, endothelial injury and microthrombi observed, particularly within the pulmonary circulation (2). Actin becomes trapped within fibrin clots in vitro, where longer actin filaments were found to increase the brittleness of clots (42, 43).

Free actin may lead to immune cell recruitment during injury. F-Actin-bound ADP, but not G actin, aggregates platelets in vitro with the effect ablated in the presence of an antibody to actin or the actin depolymerizing enzyme DNase I. Per mole of F-actin, there is one mole of bound ADP, which may provide sites for cellular interaction (44). Gold surface immobilized filamentous actin binds complement factor 1q (C1q) leading to platelet adhesion and is postulated to be a potential concern if F-actin accumulates between bodily fluids and biomaterials during medical device installation, procedures associated with tissue injury (45).

As mentioned, free actin may serve as both a disease biomarker *and* contributor to disease progression. Cytoplasmic actin protein isoforms 1 and 2 (Actin β, Actin γ) were elevated in the postshock mesenteric lymph (PSML) of a hemorrhagic shock (HS) rodent model (24). In another HS rodent model, Actin, γ, cytoplasmic 1 ^{R4} (Actg1) again demonstrated one of the greatest fold increases, as well as highest number of protein-protein interactions under proteomic analysis (26). Actin cytoplasmic 2 and actin α cardiac muscle 1 were detected in the PSML of trauma patients (25). Importantly, HS is characterized by gut ischemia, intestinal hypoperfusion and gut barrier failure, and is linked to subsequent ARDS and multiple organ failure (MOF). A proposed conduit of disease progression is a mesenteric lymph (MS) route for gut-sourced toxic factors and bacteria (24-26, 46). ATP depletion during hypoperfusion is believed to activate the actin-depolymerizing protein cofilin (AC), which disrupts F-actin filaments stabilizing intestinal epithelial tight junctions (TJs), thus driving gut barrier loss and inflammation following HS. In an HS rodent model, cleavage and loss of intestinal F-actin was reported within the ileum, as was increased G-actin, increased AC protein, claudin 3, and decreased TJ protein, ZO-1. In this way not only do actin and actin-interacting proteins signal disease, they play an integral role in its advancement (46).

The Extracellular Actin Scavenger System and Plasma Gelsolin

A highly conserved, homeostatic mechanism to depolymerize, sequester and clear free actin and thus ameliorate injury exists. The extracellular actin scavenger system (EASS) is comprised of two actin-binding plasma proteins, plasma gelsolin (pGSN) and group-specific protein (Gc) protein (58 kd). The capacity of the system can be exceeded in times of great injury however (2).

Hypogelsolinemia occurs in many clinical conditions and correlates strongly with outcome. Low GSN levels in the plasma are observed in patients with sepsis (47), ARDS (4), rheumatoid arthritis (RA) (48), severe trauma (49), *Plasmodium falciparum* malaria (50), burns (23) and following allogeneic hematopoietic stem cell transplantation (HSCT). Levels of pGSN may also be predictive for idiopathic pneumonia syndrome (IPS), often fatal after transplant, and pGSN replacement may prevent or treat IPS (51). As pGSN is a normal plasma component, its repletion via infusion or inhalation may provide a safe intervention. pGSN may therefore serve as a prognostic biomarker and therapeutic agent (50-52).

Plasma Gelsolin Biochemistry and Function

GSN is a highly conserved multifunctional actin-binding protein first discovered in macrophage cytoplasm by its actin-severing abilities (53). It has two splice variants, a cytoplasmic (80 kd) and secreted (83 kd) form (54), both functional and encoded by a single gene (55, 56). pGSN differs from cGSN by the addition of a 25-amino acid N-terminal extension (56). pGSN is secreted by muscle, with message found in human fibroblasts, macrophages and others (57). It is abundant in human plasma and is present around 220 mg/L with a half-life of 2.3 days (58). pGSN is a single chain protein comprised of 6 homologous domains connected by linker regions with modulation by Ca^{2+}, pH and phosphoinositides (PPIs) such as phosphatidylinositol-4,5-bisphosphate (PIP_2) (59). GSN has three distinct actin-binding sites and under micromolar levels of Ca^{2+}, nonproteolytically severs filaments of actin by breaking actin-actin bonds between adjacent monomers. It then caps them stably at the barbed end ($1x10^{-9}$ mol/L association constant) forming an Actin-Gelsolin complex, thus preventing further addition of G-actin monomers (60, 61). GSN capping of severed actin filaments is disrupted by PIP_2 and

filament severing is inhibited when PIP_2 is bound (3, 60, 62, 63). To a lesser degree GSN alone or in complex with actin also engages in actin filament nucleation of G-actin monomers (3, 64).

The Extracellular Actin Scavenger System and Group-Specific Protein

Both pGSN *and* Gc-protein are required for proper functioning of the EASS. pGSN alone cannot scavenge excessive amounts of F-actin without G-actin monomer saturation occurring. Effective depolymerization of F-actin is reliant on availability of *both* functional pGSN and Gc protein (65). Primarily a plasma protein synthesized in the liver (66), Gc protein is an α-2-globulin that binds noncovalently and avidly to G-actin ($1\text{-}10x10^{-8}$ mol/L association constant) at a stoichiometric ratio of 1:1 (67, 68). One of several multifunctional actin-binding proteins, it was originally known as vitamin D-binding protein (VDBP) due to its transport of vitamin D metabolites (69). Relatively well conserved, the absence of Gc protein is suspected to be fatal (70). It has a half-life of 12 to 24 hours and is found at higher concentrations in the plasma than pGSN (350-550 mg/L) (3, 66). Gc protein binds and sequesters G-actin with greater avidity than pGSN, freeing pGSN for critical F-actin severing and capping which it cannot do when bound with G-actin monomers. Scavenged complexed actin is then cleared from plasma by the liver (3, 71-73). Gc protein:Actin complexes are more rapidly cleared than pGSN:Actin complexes (3, 72, 73), yet both proteins can become depleted during overwhelming actin release. As with pGSN, septic patients also display low Gc protein plasma levels and elevated Gc protein:Actin complexes. The percentage of Gc-Actin complexes strongly correlates with disease severity and poor clinical outcome in septic shock (27) and fulminant hepatic necrosis (28, 29).

Lung and Tissue Injury Lead to Increased Risk of Infection

Bacterial infections are common in inflamed lungs. Patients suffering from acute lung injury (ALI) are more prone to infection (7), observed by high rates of ventilator-associated pneumonia (VAP) in burn inhalation injury patients for example (6). Seasonal and epidemic influenza (9, 74-80) as well as other respiratory viruses such as rhinoviruses, adenoviruses, respiratory syncytial virus (RSV), human parainfluenza viruses and measles virus, have long been associated with subsequent secondary bacterial pneumonias (81). Secondary bacterial pneumonia during the 1918 influenza pandemic, due predominantly to infection with the less invasive *S. pneumoniae,* is now known to have accounted for a much greater degree of observed mortality, (74, 77, 79) with some 50 million persons believed to have died from pneumonia due to co-infection (79). These findings underscore growing concerns surrounding rising antibiotic resistance, newly emerging bacterial strains as culprits in co-infection, incomplete coverage by the current pneumococcal conjugate vaccine, increased community carriage of pneumococcal bacteria and the high number of influenza viruses incubating in bird reservoirs. They point also to the very great need for new potential immunomodulators such as pGSN to supplement existing prophylactics and treatments.

A multitude of mechanisms accounting for the increased risk of bacterial infection in inflamed and injured lungs have been investigated (82, 83). Respiratory epithelial cell damage, alterations to epithelial cell surface receptors, basement membrane damage and exposure (84, 85) and reduced mucociliary transport have all been proposed to weaken host defenses (86). Altered behavior in resident alveolar and exudate macrophages (87-89), neutrophils (90) and NK cells (9) have also been attributed to increased infection risk, as have alterations in cytokines and

chemokines during viral infection (9, 90, 91). Our lab recently demonstrated enhancement of macrophage NOS3 with pGSN in a murine model of primary and postinfluenza secondary pneumonia. We observed improved macrophage uptake and killing of bacteria, reduced acute inflammation and improved mouse survival (5). As pGSN is a critical actin-scavenging protein, inflamed lungs are more prone to bacterial infection and free actin is present in injured lungs and increasingly viewed as detrimental, we sought to assess the effects of free actin on lung macrophage bacterial defenses.

Questions Addressed in Thesis

1. Can we demonstrate free actin release in a number of murine and human lung injury models?
2. Is host defense impaired in vivo in a murine model of lung injury characterized by free actin release?
3. Are alveolar macrophage host defenses impaired in the presence of free actin and is this reversed with pGSN?
4. What is a mechanism by which free actin interferes with normal alveolar macrophage function?

Chapter 1

Free Actin Impairs Macrophage Bacterial Defenses via Scavenger Receptor MARCO Interaction, with Reversal by Plasma Gelsolin

Christine M. Ordija[1], Terry Ting-Yu Chiou[1], Zhiping Yang[1], Glen M. Deloid[1], Melina de Oliveira Valdo[1], Zhi Wang[1], Sally A. Bedugnis[1], Terry L. Noah[3], Samuel Jones[3], Henry Koziel[4], Lester Kobzik[1]

[1]Department of Integrative and Molecular Physiological Sciences, Harvard T.H. Chan School of Public Health, Boston, Massachusetts
[2]Division of Nephrology, Department of Internal Medicine, Kaohsiung Chang Gung Memorial Hospital, Chang-Gung University College of Medicine, Kaohsiung, Taiwan
[3]Department of Pediatrics, Pediatric Pulmonary Division, University of North Carolina at Chapel Hill, Chapel Hill, North Carolina
[4]Division of Pulmonary, Critical Care and Sleep Medicine, Beth Israel Deaconess Medical Center, Boston, Massachusetts

Keywords: actin, plasma gelsolin, alveolar macrophages, scavenger receptors

Abstract:

Various lung injuries have the potential to release intracellular actin into the alveolar milieu, and are also associated with increased susceptibility to secondary infections. We investigated the effect of exposed free actin on lung macrophage host defense functions. Western blot analysis demonstrated free actin release into the lung lavage fluids of mouse models of ozone injury, influenza infection and secondary pneumococcal pneumonia, and in samples from patients following burn and inhalation injury. Using levels comparable to those observed in lung injury, we found that free actin markedly inhibited murine lung macrophage binding and uptake in vitro of *S. pneumoniae*, *S. aureus* and *E. coli* (mean % inhibition, actin vs vehicle: 85 ± 0.3 (SD), n = 22, $p < .001$). Similar effects were observed on the ability of primary human macrophages to bind and ingest fluorescent *S. aureus* (~75 % inhibition). Plasma gelsolin (pGSN), a protein that functions to bind and cleave actin, restored bacterial binding and uptake by both murine and human macrophages. Scavenger receptor inhibitors reduced binding of fluorescent actin by murine macrophages (fluorescence index ($\times 10^{-3}$) respectively after incubation with vehicle, actin, or actin + polyinosinic acid: (0.8 ± 0.7, 101.7 ± 50.7, 52.7 ± 16.9, n = 5-6, $p < 0.05$). In addition, actin binding was reduced in a MARCO / SR-AI/II deficient cell line and by normal AMs obtained from MARCO -/- mice. After release from injured cells during lung injury, free actin likely contributes to impaired host defense by blocking scavenger receptor binding of bacteria. This mechanism for increased risk of secondary infections after lung injury or inflammation may represent another target for therapeutic intervention with pGSN.

Introduction:

Injury and inflammation make the lungs more susceptible to bacterial infections. Bacterial superinfections are common following acute lung injury (ALI) (7), e.g. the ventilator-associated pneumonia (VAP) frequently observed in burn patients suffering inhalation injury (6). Similarly, influenza viral infection has long been associated with secondary pneumonias (8, 9) due predominantly to superinfection with *Streptococcus pneumoniae* or *Staphylococcus aureus* (9). Specific examples include the significant morbidity and mortality from bacterial pneumonias associated with the 1918 (74, 75, 78, 79), 1957 (80) and 1968 (76) influenza pandemics. Multiple other respiratory viruses are also linked with elevated incidence of secondary bacterial pneumonias, including measles virus, human parainfluenza viruses, adenoviruses and rhinoviruses (81).

There are multiple immunological mechanisms for increased susceptibility of injured and inflamed lungs to bacterial infection (82, 83). Impaired mucociliary transport (86), respiratory epithelial cell damage, basement membrane exposure, and viral alteration of epithelial cell surface receptors may all play a role in promoting bacterial adhesion and entry (84, 85). Impairment of leukocyte recruitment and/or activation has been reported in secondary pneumonias, with alterations observed in neutrophils (90), NK cells (9), resident alveolar macrophages (AM) and exudate macrophages (87-89). Dysregulation of cytokines and chemokines during primary influenza infection and secondary bacterial challenge may further account for predisposition to secondary pneumonias in virally infected or injured lungs (9, 90, 91).

In murine models of primary and secondary postinfluenza pneumococcal pneumonia we recently reported that plasma gelsolin (pGSN) improves host defense by enhancing lung

macrophage nitric oxide (NO) synthase type III (NOS3) function (5). However, this observation of a host defense role for pGSN indirectly also suggests another possible mechanism by which lung injury might impair host defense against infections. While having known anti-inflammatory properties via inflammatory molecule sequestration, the primary role of pGSN is as an actin scavenging protein (53).

Comprising the framework of the cytoskeleton, actin is critical for cell motility, size and shape and is the most plentiful protein in mammalian cells. Its release, however, from necrotic cells into the circulation or extracellular fluid can be damaging (3, 4). Evidence for deleterious effects of free actin include the finding that intravenous injection of G-actin monomers is fatal in rats at high concentrations with intravascular actin filament (F-actin) formation, endothelial injury and microthrombi observed, particularly within the pulmonary circulation (2). Notably, free actin has been identified as abundant or increased in a variety of injury states, having been found in postshock mesenteric lymph (PSML) in a rodent model (24), a hemorrhagic rodent model (26), and in the PSML of trauma patients (25). Actin release has also been observed in plasma in ARDS (4, 32), septic shock (27), hepatic necrosis (28, 29), some complicated pregnancies (30), severe cases of Plasmodium falciparum malaria (31), as well as in burn wound fluid (23) and sputum samples from patients with cystic fibrosis (92). Actin was differentially expressed in the bronchoalveolar lavage (BAL) fluid of ARDS patients and clearly seen to rise and fall over the course of the disease (1).

Alveolar macrophages are the initial cellular defense against bacterial infection (93-95). The finding that an actin-scavenging molecule (pGSN) can improve bacterial clearance (5) suggested that free actin released from damaged cells might directly impair macrophage-mediated bacterial clearance. We thus sought to test the potential of free actin to impair alveolar macrophage host

defense functions. Our strategy began by investigating the presence of released free actin within the lung lavage fluids of murine models of injury and infection and in human lung injury. We then measured the effect of free actin on binding and bacterial uptake by macrophages using a panel of qualitative and quantitative bacterial binding assays. Free actin caused substantial impairment of macrophage binding of bacteria. This phenomenon could be reversed by plasma gelsolin and was linked mechanistically to interactions with the macrophage scavenger receptor MARCO.

Materials and Methods

Animals:

Experiments were approved by the Harvard Medical Area Institutional Animal Care and Use Committee. Eight to twelve week old male and female C57BL/6 wild-type (WT) mice were purchased from Charles River Laboratories (Wilmington, MA) or Jackson Laboratories (Bar Harbor, ME). Eight to twelve week old female mice deficient in the scavenger receptor MARCO ($MARCO^{-/-}$) were obtained from a maintained breeding colony generated via homologous recombination and backcrossed onto the C57BL/6 background (96). Age-matched female C57BL/6 mice served as controls for those experiments using $MARCO^{-/-}$ mice. Unless specifically noted, mice utilized were eight to twelve week old male C57BL/6 WT animals. All animals were housed in a barrier facility within sterile microisolator cages, exhibited no evidence of spontaneous infection and were given a minimum 7-day acclimation period prior to experiments.

Mouse Models of Lung Injury:

Acute Ozone Exposure. BAL fluid from acute and subacute ozone exposed CPE^{fat} mice, a diabetic phenotype exhibiting spontaneous mutation in the *fat* gene, backcrossed onto the C57BL/6 background, was generously provided by Dr. Stephanie Shore. Male CPE^{fat} mice aged eleven to thirteen weeks were exposed to 0.3 parts/million (ppm) subacute ozone (O_3) for 48 h or 2 ppm acute ozone (O_3) or filtered air control for 3 h (97). Four and 24 h following exposure to acute O_3 or air control and at the end of 48 h of subacute O_3 exposure, BAL fluid was collected, carefully centrifuged to remove cells and frozen for later Western Blot analysis of free actin (98).

Influenza Model. A murine-adapted strain of influenza virus, A/Puerto Rico/8/1934 (H1N1), was purchased from ViraSource (RTP, NC). Mice were anesthetized with 120 mg/kg ketamine

plus 16 mg/kg xylazine (Vedco, St. Joseph, MO) administered via intraperitoneal (i.p.) injection. Mice then received on day 0 an intranasal instillation (i.n.) of 25- or 50-μl suspension of PBS containing varying amounts (PFUs) of APR8/34 or vehicle alone. On days 2, 5 and 7 post-influenza infection, mice were sacrificed via lethal overdose of i.p. sodium pentobarbital (Fatal-Plus, Vortech Pharmaceuticals, Dearborn, MI). In order to assess free actin release within the injured lung, bronchoalveolar lavage (BAL) was performed. The proximal trachea of euthanized mice was cannulated using a flexible 22-gaugue catheter and lungs were gently flushed with 0.6mL of cold phosphate-buffered saline (PBS). The initial lavage fluid was retained, centrifuged cold and separated from BAL cells for later Western Blot analysis of free actin (98).

Postinfluenza Pneumococcal Pneumonia. Mice were anesthetized as above and i.n. infected with 1x PBS containing varied doses of APR8/34 (0.1, 1, 3.5 and 7.5 hemagglutinating units (HAU)) on day 0. On day 7, when susceptibility to secondary bacterial challenge has been observed to be the greatest (90), mice received *Streptococcus pneumoniae* serotype 3 (American Type Culture Collection) (100, 700 or 1000 CFU i.n.) prepared as described previously (98). BAL fluid was collected for Western Blot analysis of actin as above.

Human Patient Tracheal Aspirates (TAs):

Bronchial washings were collected as previously described (99) from patients with inhalation injury and burns admitted to the North Carolina Jaycee Burn Center at the University of North Carolina at Chapel Hill (UNC) under a protocol, approved by the UNC Biomedical Institutional Review Board. Fluid was retained, centrifuged cold and separated from resident cells. BAL fluid from normal healthy volunteers was obtained as in (98), under a protocol approved by the institutional review board, and additionally concentrated for 5 minutes using the Vivaspin 6

Centrifugal Concentrator at 3000xg (Sigma-Aldrich, St. Louis, MO) for later Western Blot analysis.

***Reagents*:**

Antibodies used include rabbit polyclonal anti-β-actin (4967) and horseradish peroxidase-conjugated (HRP) secondary (Cell Signaling Technologies, Danvers, MA), rabbit polyclonal anti-Staphylococcus aureus (ab20920) (Abcam, Cambridge, UK) and F(ab′)2-goat anti-rabbit IgG (H+L) Alexa Fluor® 647 conjugated secondary antibodies (ThermoFisher Scientific, Waltham, MA). Recombinant human plasma gelsolin (rhu-pGSN) was prepared as in Lee *et al*., (2007) (100). pGSN and diluent control was provided by BioAegis Therapeutics (Morristown, NJ). Additional reagents or kits include the colorimetric Bradford Protein Assay (Bio-Rad Laboratories, Hercules, CA), TBS SuperBlock (Thermo Fisher Scientific), NuPAGE sample loading buffer (Invitrogen, Carlsbad, CA), actin protein (>99% pure) from rabbit skeletal muscle (AKL99) (Cytoskeleton, Denver, Colorado), Fc receptor blocking Human TruStain FcX™ (BioLegend, San Diego, CA), cytochalasin D, polyinosinic acid (PolyI) and dextran sulfate (Sigma-Aldrich, St. Louis, MO). Cell Mask Blue, Hoechst 33342 (Life Technologies), far red fluorescent Alexa Fluor 647 conjugated actin from rabbit skeletal muscle (A647-Actin) (A34051) and Alexa Fluor 647 conjugated albumin from bovine serum albumin (A647-BSA) (A34785) (Molecular Probes) were purchased from Thermo Fisher Scientific.

Western Blot Analysis:

Western blot analysis was performed on cell-free BAL fluid and TA in 4x NuPAGE sample loading buffer containing 9% β-mercaptoethanol according to denaturing protocols described elsewhere (101). PVDF blots were probed with 1:1000 anti-β-actin in TBS SuperBlock overnight at 4°C. Following incubation with 1:10,000 goat anti-biotin-HRP-conjugated

secondary antibody (2.5 h, room temperature) labeling was detected via luminol-based development with imaging (Alpha Innotech Imager). Quantitation was conducted using ImageJ (https://imagej.nih.gov/ij/).

Cell Isolation, Differentiation and Culture:

B6 Cell Line. Alveolar macrophages obtained from normal male C57BL/6 mice were immortalized *in vitro* via infection with a recombinant J2 retrovirus positive for *v-raf* and *v-myc* oncogenes using the method reported in (102).

ZK (SR-AI/II and MARCO-deficient) Cell Line. Similarly, the J2 retrovirus was utilized to create an immortalized alveolar macrophage line deficient in SR-AI/II and MARCO scavenger receptors (SRs) obtained from double-deficient MS-/- mice (102). B6 and ZK cell lines were cultured in RPMI 1640 medium (+L-glutamine) (Gibco, Thermo Fisher Scientific) with 25mM HEPES (Lonza, Portsmouth, NH) supplemented with heat-inactivated 10% FBS (Atlanta Biologicals, Flowery Branch, GA) and penicillin-streptomycin (Corning, Corning, NY) at 37°C, 5% CO_2. PCR confirmation of ZK cell SR-AI/II and MARCO deficiency compared to B6 cells was conducted (102). Both lines were also demonstrated via the Mycoplasma PCR ELISA test to be Mycoplasma-free (Roche, Indianapolis, IN.)

Primary GM-Mϕs. Human peripheral blood and monocyte-derived, granulocyte and macrophage-colony stimulating factor (GM-CSF)-matured macrophages were prepared (103). The Kraft Family Blood Donor Center at the Dana Farber Cancer Institute (Boston, MA) or New York Biologics (Southampton, NY) supplied buffy coats that were harvested and enriched for monocytes with the RosetteSep Monocyte Enrichment kit (Stem Cell Technologies, Vancouver, BC, Canada). Monocytes were then cultured for 11 days at 37°C, 5% CO_2 in Vuelife bags

(American Fluoroseal, Gaithersburg, MD) in RPMI supplemented with 10% FBS, 20 μg/mL gentamycin and 20 ng/mL GM-CSF (Peprotech, Rocky Hill, NJ) (103).

Bacterial Culture: *Streptococcus pneumonia* serotype 3, *Escherichia coli* and *Staphylococcus aureus* were purchased from American Type Culture Collection (ATCC, Rockville, MD) (#6303, 19138 and 25923 respectively) and were cultured at 37°C overnight on 5% sheep blood infused tryptic soy agar (TSA) plates (#90001-282, VWR, West Chester, PA) (5). *S. pneumoniae* was incubated at 37°C overnight until reaching mid-log phase (16hr) and collected in suspension in PBS. OD_{600} values were used to estimate bacterial suspension concentrations based on past standard curve preparation with actual bacterial concentration additionally confirmed via CFU from overnight culture (5, 98). Similarly, *E. coli* and *S. aureus* preparation was conducted as outlined in (98).

Green fluorescent protein (GFP)-*Staphylococcus aureus* (strain RN6390) was the generous gift of Dr. Ambrose Cheung (Dartmouth Medical School, Hanover, NH, USA). A 0.5mL -80°C frozen stock was quickly thawed and added to 10mL of Tryptic Soy Broth (TSB) and a GFP-positive RN6390 selection agent (2.5 μg/mL chloramphenicol) in a loosely capped 50mL conical with outer safety vessel. Bacteria were incubated for 4 hours at 37°C with shaking (250 rpm). Bacteria were washed twice in cold 1xPBS (-Ca,-Mg) via centrifugation. Pelleted bacteria were resuspended in PBS and filtered through a 5μM syringe filter. CFU estimates were generated from OD_{600} values and prior standard curves as reported (104).

Actin Preparation:

Rabbit skeletal muscle actin (AKL99, Cytoskeleton, Denver, CO, USA) was removed from -80°C, centrifuged briefly (13,000 rpm, 4°C, 3 minutes) and allowed to come to 4°C over approximately 30 minutes. Actin was gently resuspended in General Actin Buffer (GAB: 5mM

Tris-HCL, pH 8.0; 0.2mM $CaCl_2$ in 0.9% NaCl), incubated on ice for a minimum of 1 hour and quantified via spectrophotometry (NanoDrop 2000, Thermo Fisher). This actin solution was tested for lipopolysaccharide content using the LAL chromogenic endotoxin quantitation kit (Pierce, Thermo Fisher Scientific).

Bacterial Binding and Phagocytosis Assay (CFU Assay):

B6 macrophage binding and internalization of *S. pneumoniae, E. coli* or *S. aureus* (CFU1) was assessed through macrophage lysis in 10-fold excess H_20 (pH 10, 3 min) via CFU assay as detailed (98). To establish the effects of an actin dose curve, in total sample volumes of 0.5mL, $0.5x10^6$ B6 cells in HBSS were mixed with 10:1 *S. pneumoniae* plus equal parts per volume graded rabbit skeletal muscle actin in GAB (0.125, 0.25 or 0.5 mg/mL) in 2mL LoBind microcentrifuge tubes (Eppendorf, Hamburg, Germany) and incubated for 1 hour at 37°C. Estimation of 10 bacteria per 1 macrophage was determined via prior CFU assessment of the bacterial suspension. Following incubation, cells were centrifuged, washed, lysed and resuspended in PBS for culture on 5% sheep blood infused TSA plates as detailed (98) to assess the total cell-associated bacterial CFU (CFU1, bound and internalized). B6 binding and internalization of *S. pneumoniae* was additionally assessed via CFU assay in the presence of 0.25mg/mL BSA or 0.25mg/mL heat-denatured actin (95°C, 5 min). CFU1 for B6 cells mixed with (10:1) gram-positive *S. aureus* or (10:1) gram negative *E. coli* and actin was also assessed. Finally, B6 cells in HBSS were mixed with (10:1) *S. pneumoniae* and 0.25mg/mL actin in GAB plus 0.25mg/mL rhpGSN followed by CFU assay.

Binding and Phagocytosis Assay with High-Throughput Scanning Cytometry Analysis:

Adherent human GM-Mϕs were resuspended at $3x10^5$ cells/mL in RPMI 1640 (+L-glutamine) supplemented with 10% FBS, 20 ng/mL GM-CSF and no antibiotics. 75,000 cells were seeded

per well in 96-well black-walled Micro-Clear plates (Greiner Bio-One, Monroe, NC) and incubated for 24 - 48 hours at 37°C and 5% CO_2 as in DeLoid *et al*., 2009 (104). 12 hours preceding the assay, cells were washed with DPBS (+$CaCl_2$, +$MgCl_2$) (Gibco) and resuspended in RPMI 1640 (+L-glutamine) and 0.5% BSA (Gibco). During the assay, $2x10^8$/mL unopsonized GFP-*S. aureus* suspended in RPMI 1640, 50% GAB and 0.05% BSA alone, with a negative control 5 μM Cytochalasin D (to block internalization), or with treatments, 0.25 mg/mL actin, 0.25 mg/mL rhu-pGSN or 0.25 mg/mL actin plus 0.25 mg/mL rhpGSN, were added to GM-Mϕs and incubated at 37°C, 5% CO_2 for 45 min. Cells were gently washed 3x with DPBS, fixed in paraformaldehyde at room temperature for 16 min and washed in PBS. For labeling of external GFP-*S. aureus*, cells were incubated overnight at 4°C in 2.5 μg/mL anti-*Staphylococcus aureus* antibody (Abcam) suspended in blocking buffer (5% human serum, 5% goat serum, 1% BSA, 1% Human TruStain FcX™ in DPBS). Cells were washed 3x in PBS, resuspended in 5 μg/mL A647-F(ab')2 goat anti-rabbit IgG (ThermoFisher Scientific) in blocking buffer and incubated overnight at 4°C. Following 2x washes in PBS, to stain dead *S. aureus*, cells were resuspended in 0.1% saponin, 50 μg/mL RNase A and 100 U/mL RNase T1 in TE buffer (pH 7.5) and incubated for 1h and 20 min at 37°C, 5% CO_2. Volume was replaced with 0.1% saponin and 1 μM SYTOX Orange in HBSS and incubated at room temperature for 20 minutes. Cells were washed 2x with PBS and incubated overnight at 4°C in 1:5000 Hoechst 33342 nuclear stain and 1:1000 Cell Mask Blue in PBS. Stains were replaced with PBS and plates were stored at 4°C until undergoing scanning cytometry. A GFP-*S. aureus* control plate was also prepared to assess background fluorescence (104).

Confocal image acquisition was conducted using a BD Pathway 855 High-Content Bioimager, AttoVision imaging software (BD Biosciences, San Jose, CA) and a 20X NA075 lens

(Olympus, Center Valley, PA) as described elsewhere (104). Three non-overlapping 20X image fields were acquired per microplate well every 1.5 μm with the stack collapsed to create one final image. Image analysis and quantification was conducted using custom MATLAB® scripts (The MathWorks, Inc., Natick, MA). The Hoechst nuclear staining emission signal was utilized to identify individual cells. Software analysis of collapsed Z stack images in turn generated cell numbers and live and dead GFP-expressing *S. aureus* bacterial numbers associated externally or internally within cells (104).

In Vitro Human GM-Mϕs Fluorescent-Actin Binding Analysis by Scanning Cytometry:

Human GM-Mϕs were seeded at 90,000 cells/well in 96-well black-walled Micro-Clear plates in culture media as above. Once adherent (2 – 3 days), if undergoing inhibitor treatment, cells were washed in DPBS (+Ca/+Mg), incubated at 37°C (40 min) with pan-scavenger receptor inhibitors, 25 μg/mL Poly(I) or 100 μg/mL dextran sulfate, and washed in DPBS. Remaining cells were washed twice in DPBS and all cells were exposed to 40 μg/mL A647-Actin, 40 μg/mL A647-BSA (Molecular Probes, Thermo Fisher Scientific) or vehicle alone (GAB, 50% RPMI 1640, 0.5% BSA) while protected from light at 4°C for 30 minutes. Cells were then washed in cold DPBS, fixed in 4% paraformaldehyde and incubated in 0.1% Saponin. Following PBS washes, cells were treated for 1 hour at RT in 1:5000 Hoechst and 1:1000 Cell Mask Blue stains and replaced with PBS in preparation for scanning cytometry using BD Pathway 855 High-Content Bioimager and AttoVision imaging software as above. The Hoechst nuclear staining emission signal was utilized to identify individual cells, while the A647 signal was used to discern cell borders, with both in combination used to achieve cell segmentation. Actin and BSA binding were assessed via the average value of A647 label fluorescence of total cell cytoplasm above baseline background staining for all cells on a given plate.

Macrophage Fluorescent-Actin Binding Quantitation by Flow Cytometry: $0.5x10^6$ B6 cells were either kept on ice or suspended in 25ug/mL of the pan-scavenger receptor inhibitor poly-inosinic acid in LoBind microcentrifuge tubes (Eppendorf), incubated at 37°C for 40 minutes and washed in cold PBS. All cells were then exposed to 20 μg/mL A647-Actin, 20 μg/mL A647-BSA (Molecular Probes, Thermo Fisher Scientific) or GAB vehicle alone for 30 minutes at 4°C protected from light. Cells were pelleted by centrifugation, washed with cold PBS and resuspended in cold PBS for flow cytometry using a BD Canto II flow cytometer. Cell analysis was conducted using BD FACSCanto clinical software and FlowJo, LLC Data Analysis Software (http://www.flowjo.com).

In some experiments, $0.5x10^6$ ZK (SR-AI/II-/-, MARCO-/-) cells were incubated with A647-Actin, A647-BSA (Molecular Probes, Thermo Fisher Scientific) or GAB alone, pelleted, washed and prepared for flow cytometry as above. For ex vivo analysis of primary murine AM binding of fluorescent actin, eight to twelve-week-old female $MARCO^{-/-}$ mice and age, gender-matched C57BL/6 mice were sacrificed via lethal overdose of sodium pentobarbital (Fatal Plus, i.p.) and underwent BAL fluid collection as above. Up to 3mL total BAL fluid was collected per mouse with gentle massage of the thorax. All fluid was maintained on ice, pooled for respective genotypes and centrifuged to separate BAL cells. Cells were gently resuspended in PBS and counted, with a small fraction undergoing cytospin to microscope glass slides for Diff-Quick (a modified Wright-Giemsa) staining (Baxter Scientific Products, McGraw Park, IL) and differential cell count confirming by morphology at least 95% alveolar macrophage content (102). $0.5x10^6$ ex vivo BAL cells were then either retained on ice or suspended in 100ug/mL of the pan-scavenger receptor inhibitor dextran sulfate in LoBind microcentrifuge tubes (Eppendorf), incubated at 37°C for 40 minutes and washed in cold PBS. Cells were incubated

with A647-Actin, A647-BSA (Molecular Probes, Thermo Fisher Scientific) or GAB alone, pelleted, washed and prepared for flow cytometry as above.

Statistical Analysis:

Significant differences between protein levels observed via Western Blotting were assessed via the Kruskal-Wallis test of multiple comparisons (Fig. 1). Total cell-associated CFU binding assay data (Fig. 2) were compared via Student's unpaired two-tailed t test or one-way ANOVA. Bacterial numbers and A647-fluorescence assessed via scanning cytometry (Fig. 3 and 4 respectively) were compared via one-way ANOVA with data presented as mean ± SEM. Flow cytometry % positive events and mean fluorescence index (percent parent x A647-fluorescence) (Fig. 5 and Fig. 6) were assessed via two-way ANOVA. Statistical significance for all comparisons was taken at P value <0.05 and unless otherwise noted all data are presented as mean ± SD. GraphPad Prism 6 was utilized for graphical presentation and data analysis throughout (San Diego, CA).

Results:

Free actin detection within injured lungs

To evaluate free actin release into the alveolar space by lung injury, we performed Western blot analysis of BAL collected from mice after acute and subacute O_3 exposures. Fig. 1A shows the presence of β-actin (45 kDa) after ozone exposure, with some mice exhibiting free actin release as early as 4 h after exposure, while levels are nearly undetectable in control mice exposed to filtered air. Similarly, after influenza infection of mice, Western blot analysis of BAL fluids demonstrated β-actin release by days 5 and 7 after initiation of infection (Fig. 1B). Notably, murine models indicate day 7 as highly susceptible to secondary bacterial infection (90). In a secondary pneumococcal pneumonia model, mice infected with *S. pneumoniae* following a mild (low inoculum) influenza infection, β-actin was again detected in the collected BAL fluid upon Western blot analysis, with greater actin levels detected in lavage fluids from mice receiving higher doses of initial viral inoculum (Fig. 1C).

Non-concentrated bronchial washings from human patients suffering mild and severe burn inhalation injuries also exhibited elevated β-actin levels, compared to samples obtained from normal healthy volunteers (concentrated for analysis due to the low protein concentration characteristic of normal BAL fluid). Total actin concentrations (μg/mL) for comparisons were extrapolated from an actin standard curve (rabbit skeletal muscle actin) (Fig. 1D-E), and show significant differences in samples from burn patients compared to healthy controls.

Free actin inhibits macrophage binding of bacteria

As lung macrophages mediate the initial innate immune response to many inhaled pathogens, we sought to determine the effects of free actin on their ability to interact with bacteria. Utilizing B6 cells, a murine lung macrophage-derived cell line, we conducted an in vitro assay focused on

bacterial binding and subsequent uptake in the presence of actin, followed by CFU quantitation of bacteria (98). Macrophages incubated for 1 h in the presence of 10:1 *S. pneumoniae* and actin exhibited reduced bacterial binding and uptake with increasing concentrations of actin (Fig. 2A). The concentrations were chosen to approximate levels estimated to be present in the alveolar milieu of injured lungs using data from Fig. 1D and E (see also discussion). Equal concentrations of a control protein, albumin (250 μg/mL), did not impair bacterial binding and uptake by macrophages (Fig. 2B). Notably, commercially acquired actin contains endotoxin (e.g., we measured 1.188 EU/mL in a 0.45mg/mL actin preparation), but heat-denatured actin failed to inhibit bacterial binding using conditions that do not diminish LPS bioactivity (95°C, 5 min). Impairment of macrophage function appears to therefore require structurally intact actin protein (Fig. 2C). Similarly, actin decreased binding of both gram-positive *S. aureus* (Fig. 2D) and gram-negative *E. coli* by B6 macrophages (Fig. 2E). Notably, addition of rhu-pGSN reversed the actin-mediated reduction of *S. pneumoniae* binding back to levels equal to or greater than those observed in cells treated with vehicle only (Fig. 2F). Improved uptake in the presence of pGSN is consistent with prior findings that pGSN enhances lung macrophage uptake and killing of bacteria (22).

To test whether these findings using murine cells extend to human macrophages, we measured the ability of free actin to impair human alveolar macrophage bacterial interactions in vitro using high-throughput scanning cytometry and fluorescence imaging. The number of bacteria bound by cells was significantly reduced by actin (Fig. 3B) compared to vehicle control (Fig. 3A), treatment with pGSN alone (Fig. 3D) or with Cytochalasin D (Fig. 3E), and this inhibition was reversed by addition of pGSN (Fig. 3C). The mean number of total bacteria for cells (combined bound and internalized) was also reduced by actin compared to vehicle control

and pGSN alone and these effects were reversed by the addition of pGSN. Addition of pGSN appears not only to reverse the inhibitory effects of actin but also increases the number of total bacteria per cell (Fig. 3F), consistent with the enhancement of bacterial uptake by pGSN previously reported (5).

Evaluation of the role of scavenger receptors

To examine the mechanism by which free actin impairs macrophage binding and uptake of bacteria, we exposed macrophages to fluorescently-labeled actin or BSA in the presence or absence of pan-scavenger receptor inhibitors, and then quantified bacterial binding using scanning cytometry and fluorescence imaging. GM-Mϕs exhibited robust binding of actin (Fig. 4A), but this was markedly decreased in the presence of scavenger receptor inhibitors polyinosinic acid (Fig. 4B) or dextran sulfate. The cells also showed much lower binding of a control protein, albumin (Fig. 4D) or vehicle control (Fig. 4C). The quantitative analysis of these qualitative results is presented in Fig. 4E.

We also exposed murine B6 macrophages in vitro to fluorescently labeled actin or BSA in the presence or absence of the pan-scavenger receptor inhibitor polyinosinic acid and analyzed binding using flow cytometry. The fluorescence index (percent positive cells x mean fluorescence of positives) observed indicates much greater binding of actin by B6 AMs (101775.87 ± 50787.50) (Fig. 5A, E) compared to BSA (22671.3 ± 24756.56), representing a 77.7% decrease (Fig. 5D, E). The pan scavenger receptor inhibitor polyinosinic acid reduced B6 binding of actin (52752.62 ± 16948.38513) by 48.2% and loss of SR-AI/II and MARCO SRAs in an immortalized alveolar macrophage line (ZK cells) resulted in 67.2% less actin binding (33373.93 ± 17258.26) (Fig. 5A, C). Similarly, the percentage of B6 cells positive for actin (68.1 ± 7.7%) was greater than that compared to cells incubated with BSA (6.4 ± 3.7%) (not shown),

actin with PolyI (32.8 ± 2.8%, 51.8% reduction), or ZK cells incubated with actin (30.3 ± 9.8%, 55.5% reduction) (Fig. 5B).

To further delineate the specific role of the MARCO scavenger receptor in actin binding, normal WT and MARCO -/- lavage cells (~95% alveolar macrophages) were exposed ex vivo to fluorescently labeled actin or BSA, with or without the scavenger receptor inhibitor dextran sulfate (DS), and analyzed by flow cytometry. The fluorescence index (percent positive cells x mean fluorescence of positives) again showed greater binding by WT ex vivo AMs of actin (161692.2 ± 20059.58) (Fig. 6A) compared to BSA (26541.47 ± 1587.90), representing an 83.5% decrease (Fig. 6B, D). Similarly, the scavenger receptor inhibitor DS reduced WT AM binding of actin (47655.73 ± 12445.53, 70.52% reduction) as did loss of the MARCO receptor in MARCO -/- ex vivo AMs (72590.8 ± 5619.92, 55.1% reduction). Ex vivo MARCO -/- AMs incubated with DS prior to actin exhibit even lower actin binding, with a FL Index of 21178.33 ± 1501.13, representing an 86.9% reduction) (Fig. 6A, C).

Figure 1. Free actin is present in lung injury. A: 4 and 24 h after acute ozone (O_3) exposure (2 ppm, 3 h), Western Blot analysis of CPE^{fat} diabetic murine bronchoalveolar lavage (BAL) shows detectable levels of β-actin (45 kDa); β-actin levels were low to undetectable 4 h after filtered air control exposure (3 h) and low after 24 h of subacute O_3 (0.3 ppm) exposure, (n = 12). B: β-actin is present in the BAL of male C57BL/6 mice by days 5 and 7 following i.n. instillation of influenza virus APR8/34, but not by day 2 or in vehicle control mice, (n = 7). C: β-actin is found in BAL from mice in secondary pneumococcal pneumonia following i.n. instillation of *S. pneumoniae* postinfluenza infection (APR8/34), with higher β-actin levels correlating with greater initial doses of APR8/34 (100 CFU *S. pneumoniae* for all mice postinfluenza infection except 0.1 HUA APR8/34, 700 CFU *S. pneumoniae*) (n = 10). D: β-actin in the bronchial washings of burn patients (*non-concentrated*) is detected, with relatively low levels observed in *concentrated* samples from healthy normal volunteers (4.6 μg protein loaded/lane) compared to an actin standard curve (rabbit skeletal muscle actin, μg/mL). E: β-actin levels of lavage fluids from burn patients are greater than in healthy normal controls, (n = 24), Mean ± SD, * P = 0.001

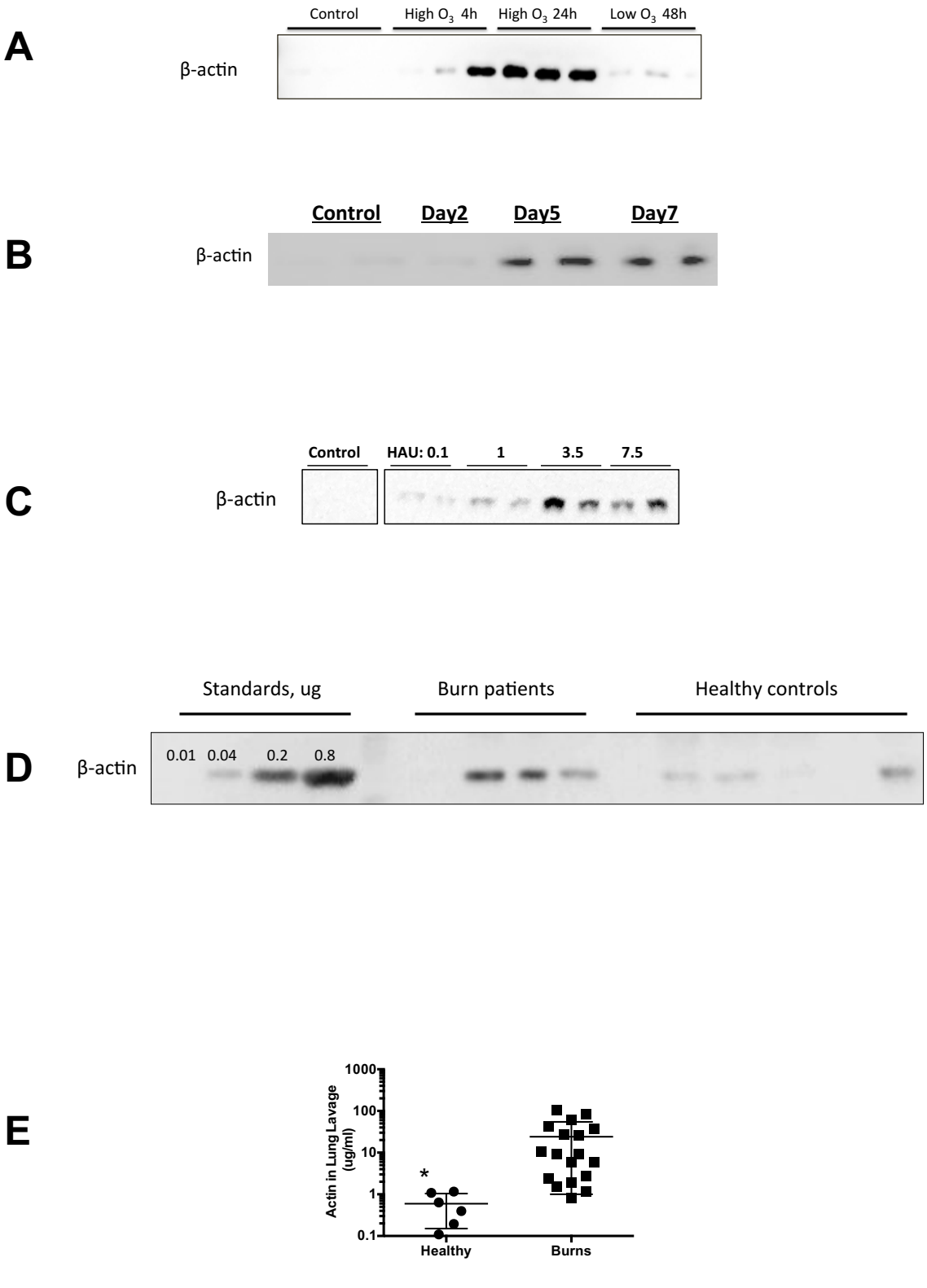

Figure 1 (Continued)

Figure 2. Free actin impairs murine alveolar macrophage binding and uptake of bacteria in vitro. Total cell-associated colony forming units (CFU) (bound and inside) following incubation of bacteria (10:1) with cells. A: Increasing actin dose (125, 250 or 500 μg/mL) decreases *S. pneumoniae* CFU (n = 16 samples) ** P = 0.005, **** P = < 0.0001. B: Equivalent albumin (250 μg/mL) did not reduce *S. pneumoniae* CFU compared to control (n = 9 samples) *** P = 0.0004, nor did C: heat-denatured actin (95°C, 5 min), although endotoxin positive (n = 2 experiments, 12 samples total) **** P = < 0.0001. D: Actin (200 μg/mL) decreased *S. aureus* CFU (n = 6 samples) ** P = 0.0058. E: Actin (200 μg/mL) decreased CFU under *E. coli* challenge (n = 5 samples) ** P = 0.0067. F: rhpGSN (250 μg/mL) added to actin (250 μg/mL) reversed reduction *S. pneumoniae* CFU (n = 2 experiments, 20 samples total) **** P = < 0.0001. All values are mean CFU ± SD. Significant differences are from control at the P values listed.

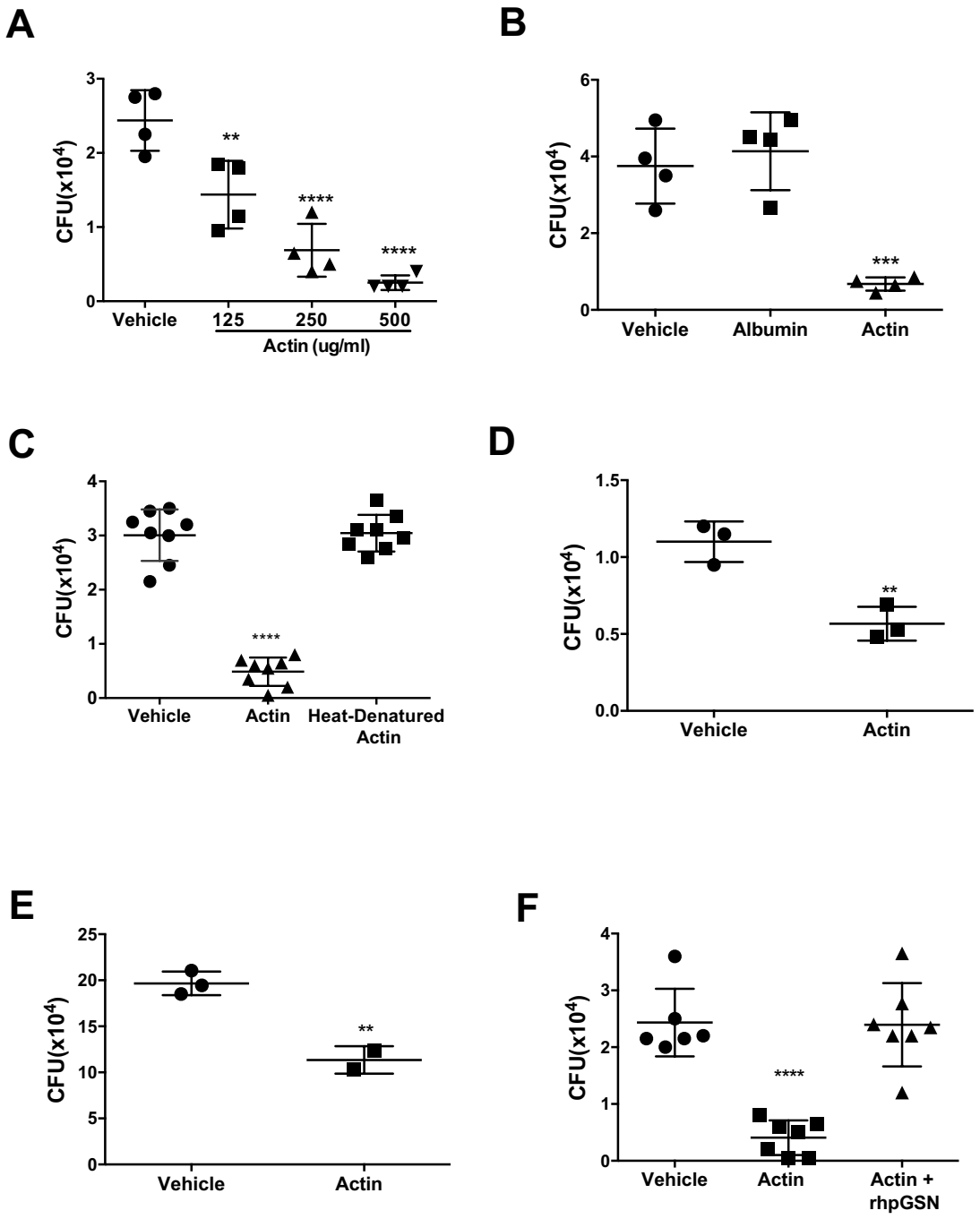

Figure 2 (Continued)

Figure 3. Free actin impairs human alveolar macrophage bacterial binding and uptake in vitro with reversal by pGSN. Binding and phagocytosis assay with scanning cytometry fluorescence imaging. Adherent human GM-Mϕs received treatments or controls during incubation with GFP-*S. aureus* (strain RN6390) (1h, 37°C, 45 min). External *S. aureus* were labeled with anti-*S. aureus* primary antibody and an Alexa Fluor 647-F(ab')2 goat anti-rabbit IgG secondary antibody. Cells were permeabilized, dead *S. aureus* were labeled with SYTOX Orange and cells with Hoechst nuclear stain and Cell Mask Blue. Representative images are merged composites of collapsed confocal stacked images: internalized live bacteria (green), internalized dead bacteria (red), bacteria bound, but not internalized (blue). A: Vehicle positive control. B: 0.25 mg/mL Actin reduces bacterial binding and uptake. C: 0.25 mg/mL Actin plus 0.25 mg/mL rhpGSN reverses inhibition. D: 0.25 mg/mL rhpGSN. E: Negative control, Cytochalasin D, bacterial internalization, but not binding, is blocked. F: Number of bound and total (bound + internalized) bacteria. All means ± SEM (n = 50 wells), Bound Bacteria: * P = 0.022. Total Bacteria: * P = 0.017 **, P = 0.001, **** P = < 0.0001

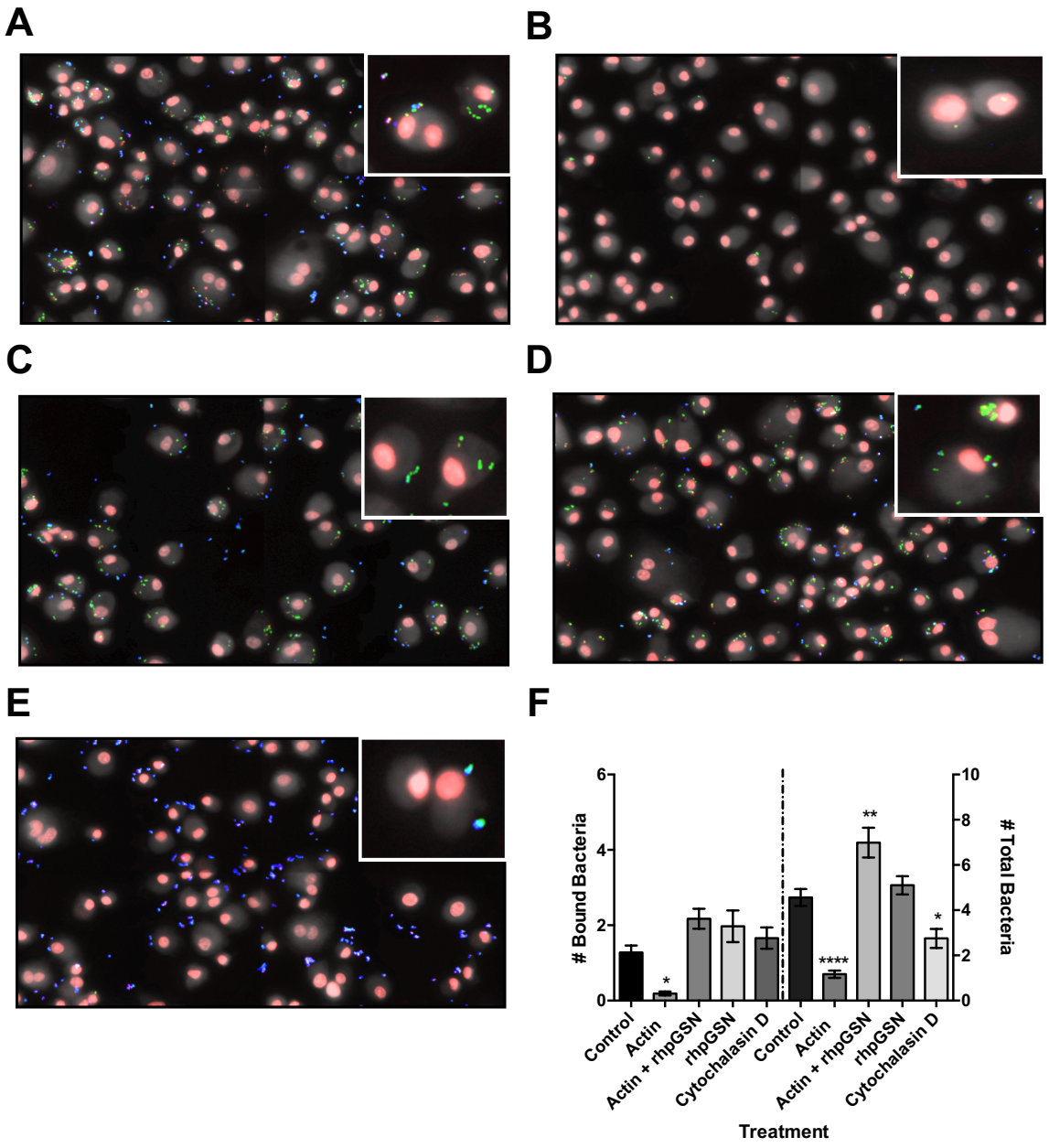

Figure 3 (Continued)

Figure 4. Free actin binds human alveolar macrophages in vitro in a scavenger receptor dependent fashion. Scanning cytometry fluorescence imaging. Human GM-Mϕs were incubated (37°C, 40 min) with or without the pan scavenger receptor inhibitor, PolyI (25 μg/mL), washed in DPBS and exposed to 40 μg/mL of AlexaFluor 647 conjugated actin from rabbit skeletal muscle, 40 μg/mL AlexaFluor 647 conjugated albumin from Bovine Serum Albumin (BSA) or vehicle alone (4°C, 30 min). Cells are labeled with Hoechst and Cell Mask Blue. Representative images are collapsed confocal stacked images. Cells incubated with A: A647-actin (n = 5 experiments, 15 wells total), B: A647-actin with PolyI (n = 2 experiments, 6 wells total), C: Vehicle control (n = 5 experiments, 15 wells total), D: A647-BSA (n = 5 experiments, 15 wells total) or E: A647-BSA with PolyI (n = 2 experiments, 6 wells total). F: Value of A647 fluorescence for total cell cytoplasm above baseline staining for all cells, showing increased binding of actin by human GM-Mϕs compared to equivalent concentrations of control protein albumin. Actin binding is significantly reduced in the presence of pan SR inhibitors. Mean FL ± SEM, **** P = < 0.0001

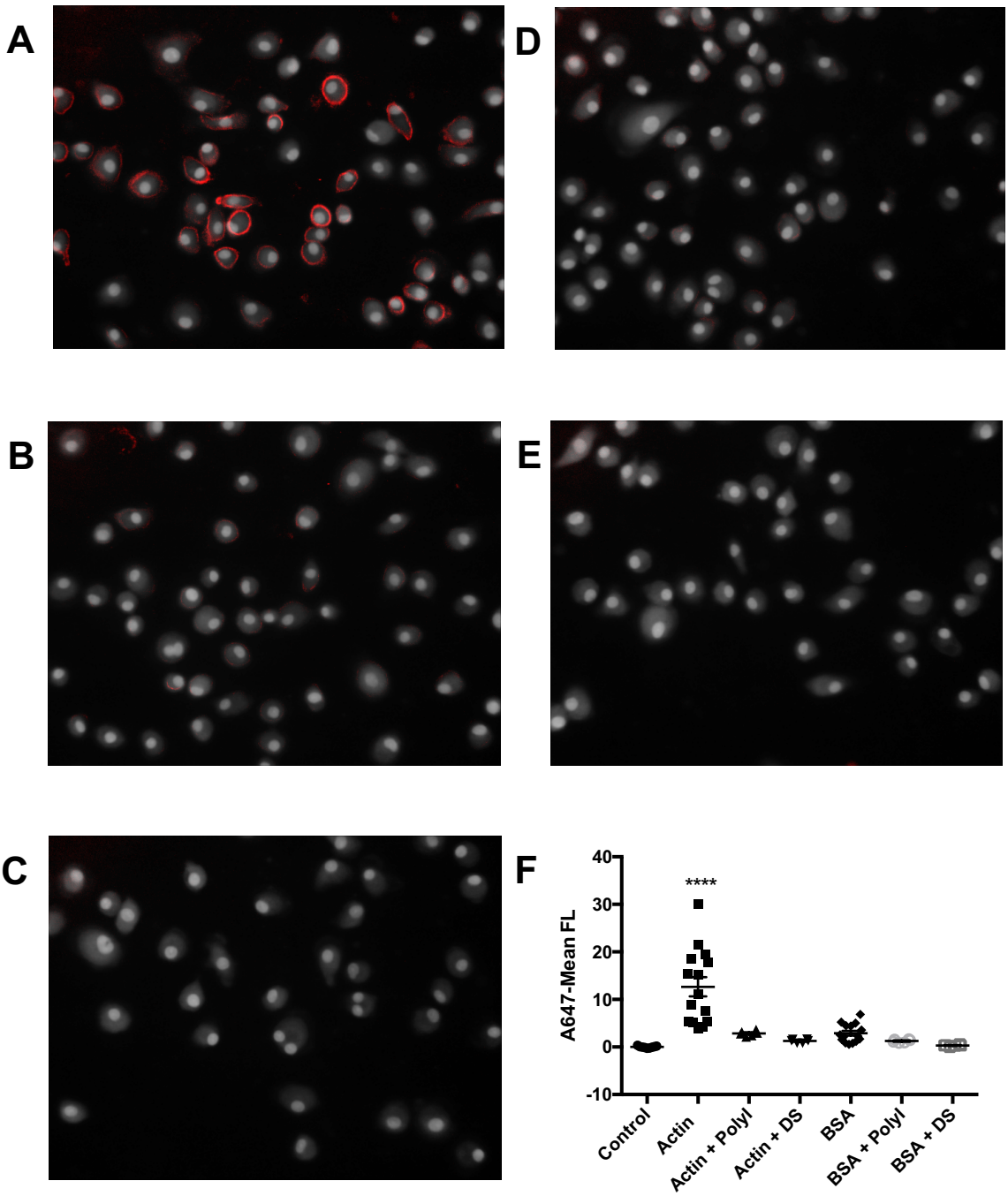

Figure 4 (Continued)

Figure 5. Free actin binds murine alveolar macrophages in vitro in a scavenger dependent fashion. B6 macrophages were pre-incubated (37°C, 40 min) with or without PolyI (25 μg/mL). B6 and ZK (SR-AI/II, MARCO -/-) AMs were then incubated with fluorescent (AlexaFluor 647) actin, fluorescent (AlexaFluor 647) Bovine Serum Albumin (BSA) or vehicle alone and analyzed by flow cytometry. A: Fluorescence index (percent positive x mean fluorescence) and B: % positive events out of 10,000 events, (n = 3 - 6) showing elevated B6 binding of actin, inhibited by scavenger receptor blocker, PolyI; * = $p < .05$ for B6-Actin vs all other groups. C: Representative histogram from experiments in A & B: Dark grey: B6 + GAB, Magenta: B6 + Actin, Green: B6 + PolyI + Actin, Blue: ZK + Actin. D: Fluorescence index shows B6 binding of BSA is significantly lower than binding of actin; * = $p < .05$ for B6-Actin vs B6-BSA. E: Representative histogram from experiments in D: Light grey: B6 + GAB buffer control, Green: B6 + BSA, Red: B6 + PolyI + BSA, Blue: ZK + BSA, Magenta: B6 + Actin. All histograms represent counts of 10,000 events per sample (n = 3 - 6)

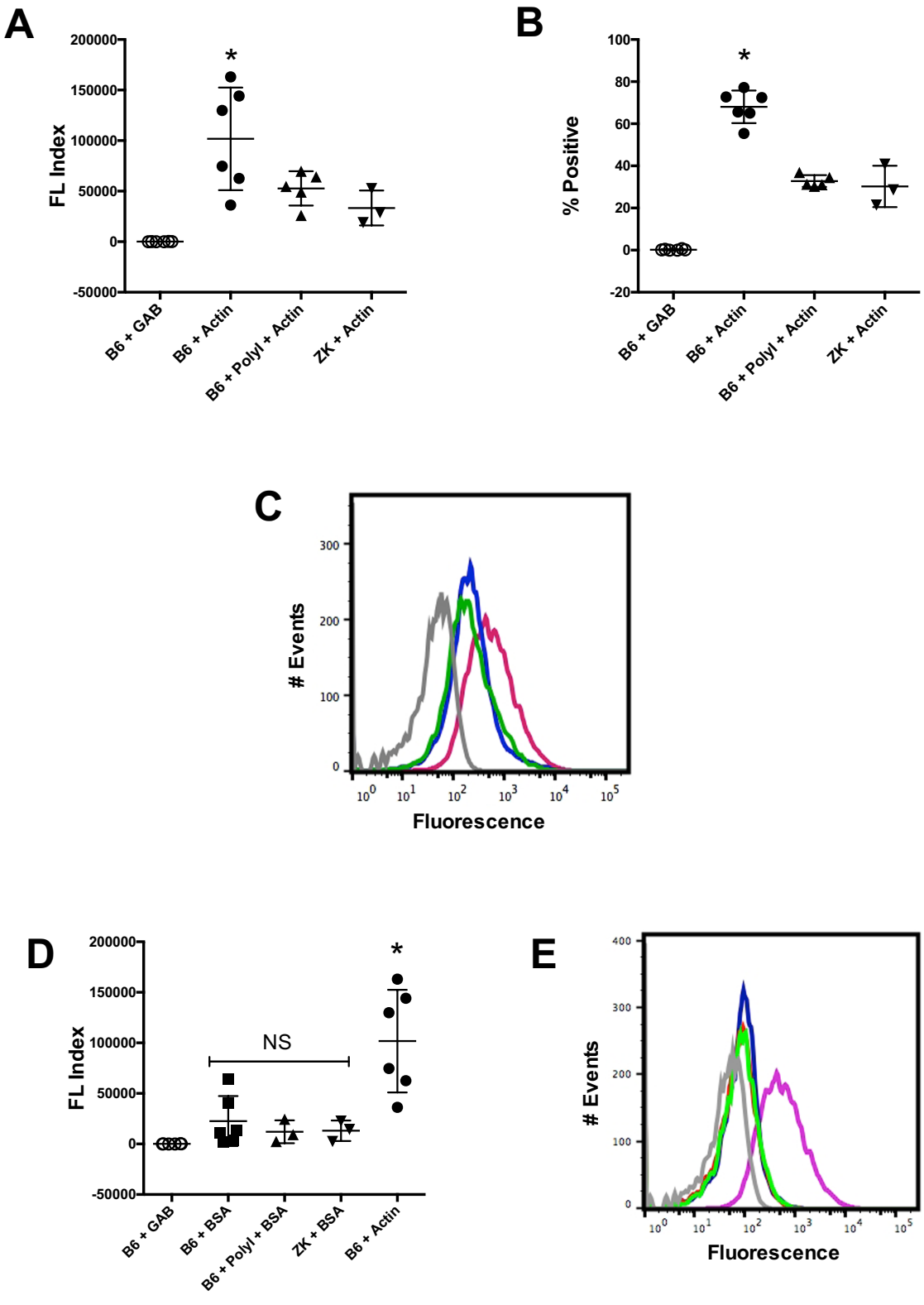

Figure 5 (Continued)

Figure 6. Actin binding mediated in part by MARCO scavenger receptor. Ex vivo WT and MARCO -/- BALF AMs were collected from lung lavage and pre-incubated (37°C, 40 min) with or without DS (100 μg/mL). AMs were washed and incubated in 20 μg/mL A647- actin, 20 μg/mL A647-BSA or vehicle alone (4°C, 30 min) and washed in preparation for flow cytometry. A: Mean fluorescence index (percent parent x A647-fluorescence) observed via flow cytometry for WT, MARCO -/- (+/- DS) with A647-Actin, B: Mean FL-Index for WT, MARCO -/- (+/- DS) with A647-BSA. C: Histograms for graph A: WT, MARCO -/- (+/- DS) with A647-Actin. Dark grey: WT + GAB, Light grey: MARCO -/- + GAB, Magenta: WT + Actin, Blue: WT + DS + Actin, Green: MARCO -/- + Actin, Red: MARCO -/- + DS + Actin. D: Histograms for graph B: WT, MARCO -/- (+/- DS) with A647-BSA. Light grey: WT + BSA, Green: WT + DS + BSA, Blue: MARCO -/- + BSA, Red: MARCO -/- + DS + BSA, Magenta: WT + Actin. All histograms represent A647-fluorescence intensity counts of 10,000 events per sample (n = 3) * $P < 0.0001$

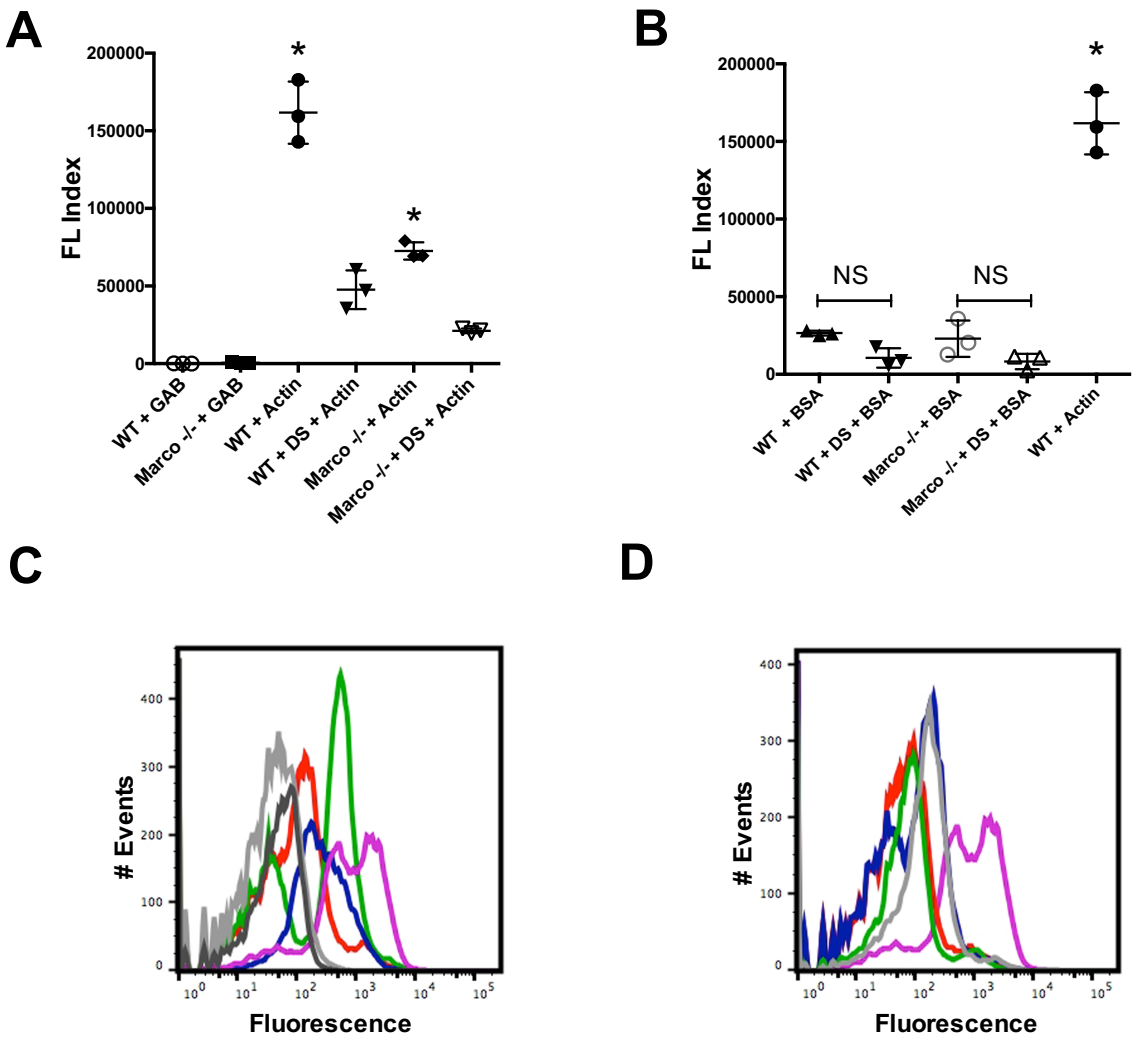

Figure 6 (Continued)

Discussion:

We sought to investigate a potential role for extracellular free actin in the impairment of alveolar macrophage host defenses against bacteria. We began by measuring free actin in the bronchial washings of patients suffering from burns and inhalation injury, as well as in murine models of oxidizing injury, influenza infection and secondary pneumococcal postinfluenza infection. These data extend prior findings of free actin in samples from injured lungs by proteomic or other methods (1, 92). Using CFU assays, scanning cytometry or flow cytometry to analyze both murine and human macrophages, we found substantial inhibition of macrophage binding for a panel of bacteria (*S. pneumoniae*, *S. aureus* and *E. coli)* by actin. The ability of free actin to impair macrophage binding of bacteria was abrogated by plasma gelsolin, a protein known to noncovalently disrupt filamentous actin (53). We have previously found that pGSN enhances lung macrophage killing of ingested bacteria by activating NOS3 (5). The data presented here indicate that therapeutic administration of pGSN may also benefit host defense by scavenging free actin; this may be especially true at time points after lung injury when free actin is detectably increased (e.g. days 5 and 7 following influenza infection, Fig 1B).

We also identified a mechanism by which actin impairs the macrophage's ability to bind bacteria. Evidence using scavenger receptor inhibitors and macrophages from mice with genetic deletion of both MARCO and SRA-I/II or MARCO alone indicated a substantial decrease in binding when these receptors were inhibited or absent. Notably, these manipulations of scavenger receptor(s) did not abolish actin binding entirely. There is likely a role for other non-SR receptor(s) or compensatory increases in SRA-I/II that account for the portion of binding that persisted in these experiments.

Some additional limitations in this study merit discussion. Other lung cells or other phagocytes (e.g. neutrophils) might also bind extracellular actin, and whether this interaction similarly impairs bacterial binding and uptake is unknown. Additionally whether macrophages bind actin in both its monomeric and polymeric filamentous forms is unknown. The commercial actin utilized in this study undergoes quality control testing to ensure it is capable of polymerizing, extracellular actin has been shown to form filaments at plasma salt concentrations (3, 4) and the great efficacy of pGSN in restoring bacterial binding and uptake by AMs in the presence of actin further points to the aggregated form of actin interacting most with macrophage receptors. Finally since commercial actin contains trace endotoxin, we evaluated the possibility of altered AM behavior due to LPS content rather than the properties of actin itself. Heat denaturation of actin, under conditions which affect actin protein structure but not endotoxin, restored normal AM binding and uptake of bacteria supporting a direct effect of actin, when intact. Bacterial and actin binding assays were conducted over short time frames further suggesting endotoxin contamination of actin to be unlikely to account for impaired AM bacterial binding in the presence of actin or macrophage scavenger receptor MARCO mediated actin binding by AMs.

Notably, pGSN has already been shown to mediate improved host resistance to infection through multiple mechanisms. pGSN counters systemic inflammation to improve survival in animal models of peritoneal bacterial infection (100, 105). Yang *et al*. demonstrated improved phagocytic uptake of bacteria in the presence of pGSN and improved bacterial clearance through pGSN enhancement of lung macrophage NOS3 (5). pGSN has been shown to be safe for use in humans (106) and may be of particular use as a therapeutic supplement to existing respiratory therapies (for patients with ARDS, secondary pneumonia, cystic fibrosis or burns and inhalation

injury) or in primary bacterial (e.g., pneumococcal) pneumonia (77). This work adds to a growing body of evidence that immunomodulatory therapy with pGSN in patients with severe flu, ARDS, burns and inhalation or other lung (or even systemic) injury may aid in the prevention of secondary pneumonia in part through its actin scavenging abilities and acts to complement earlier work conducted by Yang *et al*. (5).

In summary, extracellular free actin release was detected in samples from human and murine lung injury. Impaired alveolar macrophage binding of bacteria was demonstrated in the presence of free actin in vitro, with restoration by the actin-scavenging protein pGSN. Functional blockade of the MARCO scavenger receptor by its binding of free actin with subsequent reduced capacity for binding and clearance of bacteria represent one mechanism by which actin interferes with AM host defenses. Removal of free actin by plasma gelsolin further underscores the therapeutic potential of pGSN to reduce susceptibility of injured lungs to bacterial infections.

Grants:

Work reported here was supported by National Institutes of Health Grants T32 HL-7118-40

Acknowledgements:

We thank Dr. Thomas Stossel for his generous and thoughtful comments on plasma gelsolin and actin interactions.

Chapter 2

Effects of Ozone on Actin and Lung Injury

Introduction:

Ground level ozone (O_3) is a ubiquitous air pollutant associated with significant morbidity and mortality, including increased susceptibility to lung infection (107-111). This project sought to assess the damaging effects of free actin release as a result of ozone-mediated cellular injury in the lung, and the potential therapeutic role of the actin-binding protein plasma gelsolin (pGSN), a critical member of the extracellular actin-scavenger system (EASS). The central hypothesis is that ozone-mediated release of free actin promotes an acute inflammatory response and causes impairment of alveolar macrophage (AM) bacterial clearance. Scavenging of damaging free actin by available or administered pGSN is in turn postulated to aid in AM immune defenses. The goal of this project was to better characterize the roles of actin and pGSN in ozone-mediated lung injury and to evaluate pGSN as a potential therapeutic in lung injury characterized by free actin release.

Public Health Impacts and Epidemiology

O_3 is an ambient oxidant gas comprised of three atoms of oxygen. While beneficial in the stratosphere, tropospheric ground level O_3 is a hazardous air pollutant and significant public health concern. In the troposphere it is primarily generated via chemical reactions between volatile organic compounds (VOCs), carbon monoxide (CO), and oxides of nitrogen (NOx) such as nitric oxide (NO) and nitrogen dioxide (NO_2) in the presence of heat and sunlight. These O_3 precursors are mostly anthropogenic in origin, derived from the incomplete combustion of fossil fuels (112-115). Despite declines in anthropogenic emissions, climate projection models predict future O_3 level increases over heavily populated, polluted and biomass burning areas (112, 116-

119), intensifying public health concerns given ongoing industrialization and rapid global urbanization (120).

Identified as a criteria air pollutant by the EPA in the Clean Air Act of 1970 (107, 110), O_3 exposure is associated with elevated morbidity and mortality (107-109, 111, 121). The young, elderly, and persons with preexisting lung conditions are particularly at risk of adverse respiratory outcomes in relation to air pollution (110, 122-124), with pregnant women and persons suffering from obesity also being populations of concern (125). Inhaled O_3 exposure is linked clinically and experimentally with lung inflammation (126), spirometric lung function decrements (127-129) and airway hyperresponsiveness (AHR) (127). Observational studies associate elevated O_3 exposure with increased susceptibility to lung infection (130), exacerbation of asthma (110, 124), chronic obstructive pulmonary disease (COPD) (131), increased pediatric respiratory-related emergency room visits (132), hospital admissions for both COPD and pneumonia (130), and in pregnant women, the incidence of pre-eclampsia and preterm birth, with the latter potentially elevated in asthmatic women (133). The current National Ambient Air Quality Standard (NAAQS) for O_3 is 0.075 parts per million (ppm), lowered in 2008 from the previous 8-hour standard of 0.08 ppm to better protect at risk populations. Kim *et al*. however induced neutrophilic inflammation and reductions in FEV_1 in *healthy* adults via 6.6 hours of moderate exercise in 0.06 ppm O_3, levels lower than the current standard (129). Furthermore many U.S. metropolitan cities are already in frequent nonattainment of the EPA standard and numerous locales internationally far exceed it.

Pulmonary O_3 Toxicity

Oxidative stress, inflammation and tissue injury are observed in the lungs of humans (126-129, 134, 135) and laboratory animals (136-141) following O_3 exposure. Toxicity is initiated as

O_3 induces peroxidation of unsaturated fatty acids in cell membrane lipids and the surfactant lining of the airways. Reactive oxygen species and lipid ozonation products generated exert oxidative stress further damaging the airway epithelium (142, 143). Disruption by O_3 of the epithelial lining tight junctions increases transmucosal permeability between the airway lumen, interstitium and blood, thus allowing serum protein transport into the lumen with the potential entry of toxic co-pollutants like particulate matter (PM) into the subepithelial compartment and circulation (136, 137, 142).

Activated epithelial cells and resident AMs produce inflammatory mediators such as the arachidonic acid metabolites, prostaglandins and leukotrienes (144), as well as inflammatory cytokines and chemokines (134, 145). Elevated prostaglandin E_2 (PGE_2), IL-6, lactate dehydrogenase (LDH), neutrophil elastase and fibronectin, all indicative of inflammation and tissue injury, are present in O_3 exposed human BAL (145). O_3 exposure induces mast cell activation (139) and lung recruitment of dendritic cells (126), monocytes (126, 146) and the hallmark response, inflammatory neutrophils (PMNs) (126, 134, 135, 146, 147). The innate immune system is activated. Oxidant damage to lung extracellular matrix liberates fragments of hyaluronan (HA) that signal through TLR4 to contribute to AHR (148). Some anti-inflammatory macrophage phenotypes are also activated. The Class A scavenger receptor (SRA) macrophage receptor with collagenous structure (MARCO) scavenges oxidized surfactant lipids (149) while late expression by AMs of heme-oxygenase-1 (HO-1) promotes wound repair (150). O_3-induced classical activation of AMs however leads to the release of cytotoxic and proinflammatory mediators like TNFα furthering tissue injury (151-153). Ozone's primary targets are the proximal alveolar regions of the lung, the bronchiole-alveolar duct junction and terminal bronchioles (154). Particular structural losses are seen among ciliated and Clara cells in the

sensitive terminal bronchioles of rats exposed to only 0.25 ppm O_3 for 12 hours (155). Epithelial cell necrosis is observed in the terminal bronchioles of juvenile rats as early as 4 hours following 1.0 ppm O_3 exposure, thus demonstrating that early necrotic events precede peak inflammatory PMN influxes (156).

O_3 Immunosuppressive Effects

O_3 exposure alters the host immune response and increases susceptibility to lung infection (107, 157, 158). Mucociliary function within the tracheobronchial airways is altered and may play a role in susceptibility (159, 160). Impaired bacterial clearance following O_3 exposure is related to reduced AM phagocytosis (157, 158, 161). PGE_2, elevated in BALF after O_3 exposure, depresses AM function and may contribute to reduced internalization (158). The normal ability of surfactant protein A (SP-A) to enhance phagocytosis is diminished once oxidized (162). AMs comprise the majority of phagocytes in the lower respiratory tract and are a critical first line of defense against inhaled pathogens (163). High incidence of pneumonia among patients exhibiting neutropenia or macrophage dysfunction underscores the significance of phagocytosis in proper host defense (164). No mention is made in the literature on the potential for free actin to impede AM phagocytosis. Our goal was thus to investigate the possibility that O_3-induced free actin release plays a role in observed impairment of macrophage host defense functions.

Materials and Methods

Animals:

Experiments were approved by the Harvard Medical Area Institutional Animal Care and Use Committee. Seven to nine week old male C57BL/6 wild-type (WT) mice were purchased from Charles River Laboratories (Wilmington, MA). All animals were given a minimum 7-day acclimation period prior to experiments.

Mouse Models of Lung Injury:

Acute Ozone Exposure. Male C57BL/6 mice aged seven to nine weeks old were exposed to 0.5, 1, 2 parts/million (ppm) acute ozone (O_3) or filtered air control for 3 h (97). Four and 24 h following exposure, mice were sacrificed via lethal overdose of sodium pentobarbital (Fatal Plus, i.p.) and underwent BALF collection. Up to 3mL total BALF were collected per mouse with gentle massage of the thorax. All BALF was maintained on ice, centrifuged to separate BAL cells and BALF. BALF was frozen for later TNFα ELISA and Western Blot analysis for free actin. Cells were gently resuspended in PBS, counted, and a small fraction underwent cytospin to microscope glass slides for Diff-Quick (a modified Wright-Giemsa) staining (Baxter Scientific Products, McGraw Park, IL) and differential cell count (5).

Acute Ozone Exposure with Aerosolized rhu-pGSN. Male C57BL/6 mice aged seven to nine weeks old were exposed to 2 ppm O_3 for 3 h followed by 30 minutes of nebulized rhu-pGSN or placebo (1mM CaCl2 in 0.9% NaCl). BALF was collected 4 and 24 h following O_3 exposure for Western Blot analysis and differential cell count as before. The above experiment was repeated with BALF collection 2 h following O_3 exposure so as not miss a potential early detectable pGSN effect.

Acute Ozone Exposure with Subcutaneous rhu-pGSN. Male C57BL/6 mice aged eight weeks old were pre-treated with rhu-pGSN (11.5mg) or placebo delivered via subcutaneous injection 26 and 2.5 h prior to acute 2 ppm O_3 exposure for 3 h. BALF was collected 4 and 24 h following O_3 exposure for Western Blot analysis and differential cell count as before.

Reagents:

Antibodies used include anti-β-actin (4967S, Santa Cruz Biotechnology, Santa Cruz, CA), horseradish peroxidase-conjugated (HRP) secondary antibodies (Cell Signaling Technologies,

Danvers, MA) and anti-hu-pGSN provided by Dr. Thomas Stossel. Recombinant human plasma gelsolin (rhpGSN) was prepared as in Lee *et al*., (2007) (100). pGSN and diluent control was provided by BioAegis Therapeutics (Morristown, NJ). Diff-Quick (a modified Wright-Giemsa) stain was purchased from Baxter Scientific Products (McGraw Park, IL).

Western Blot Analysis:

Total protein concentration of BALF was assessed via the colorimetric Bradford Protein Assay (Bio-Rad Laboratories, Hercules, CA). BALF was combined with 4x NuPAGE sample loading buffer containing 9% β-mercaptoethanol and heated at 72° for 15 minutes (101). Proteins were separated in MOPS SDS running buffer under denaturing conditions via gel electrophoresis (NuPAGE 4-12% Bis-Tris gel, 1.0 mm, 10-15 well) using the NuPAGE Electrophoresis System (100 constant volts, 2.5 h) (Invitrogen, Carlsbad, CA). Proteins were transferred to PVDF membrane in the presence of NuPAGE transfer buffer plus 20% methanol overnight (70 constant milliamps, 4°C). Blots were rinsed briefly in 1X Tris-Buffered Saline (TBS) and blocked in 1X TBS/0.01% Tween-20 (1X TBS-T) and 5% w/v milk for 2 h rocking gently at room temperature. Following washes in 1X TBS-T (3x 5 minutes each, rocking), blots were probed with 1:1000 anti-β-actin or anti-hu-pGSN in TBS SuperBlock (Thermo Fisher Scientific) overnight at 4°C. Following washes as described above, blots were incubated for 2.5 h rocking at room temperature in 1:10,000 goat anti-biotin-HRP-conjugated secondary antibody in 1X TBS-T plus 1% w/v milk. Following 3x 15-minute washes in 1X TBS-T with rocking at room temperature, blots underwent luminol-based development and imaging (Alpha Innotech Imager).

Statistical Analysis:

Significant differences were assessed via Student's unpaired two-tailed t test or one-way ANOVA. Data are presented as mean ± SD and statistical significance was taken throughout at P

value <0.05 with GraphPad Prism 6 utilized for all graphical presentation and data analysis (San Diego, CA).

Results:

Mice exposed to acute O_3 exhibited increased polymorphonuclear neutrophil influx compared to filtered air control mice, consistent with lung injury. This response was generally dose-dependent, however significant variability in PMN levels were observed between individual mice exposed to comparable doses of O_3 (Fig. 7A). Elevated total protein concentrations are observed in all groups except 0.5 ppm acute O_3 exposed mice and are indicative of increased transmucosal permeability, consistent with lung injury (Fig. 7C). While an increasing trend in levels of TNFα, a cytokine marker of inflammation, was present in the BALF of O_3 exposed mice, differences between acute O_3 and filtered air control mice were not statistically significant (Fig. 7D). Western Blot analysis of BALF from mice exposed to acute O_3 (3 h) compared to filtered air controls revealed the presence of free actin indicative of lung injury (Fig 7E).

From these ozone dose response results, exposure to 2 ppm O_3 was deemed to induce sufficient injury for the assessment of free actin release and pGSN effects, while lower doses were not. The actin-scavenging protein pGSN was administered to test the potential benefits of removing excess free actin released during ozone-mediated lung injury. Mice receiving rhu-pGSN delivered via nebulization after acute O_3 exposure did not however show any benefit compared to placebo treated animals. No significant reductions in PMN influx via cytospin (Fig. 8A-B) or total protein (Fig. 8C) and free actin in the lung, as observed via Western blotting in BALF collected 4 h after O_3 exposure (Fig. 8G), were observed. Similarly, subcutaneous treatment with rhu-pGSN prior to acute O_3 exposure also failed to measurably reduce lung injury in mice compared to animals receiving placebo (Fig. 9A-C).

Figure 7. Ozone induces lung injury with free actin release. BALF collected from male C57BL/6 mice 4 and 24 h after 0.5, 1, 2 ppm acute O_3 or filtered air control exposure (3 h). A: Differential cell count of BALF following cytospin showing % PMN influx and B: total # of PMN (x10K). C: BALF total protein (mg/mL) (n = 63) and D: TNFα (pg/mL) from ELISA (n = 26) E. Western Blot analysis for free actin (42 kDa, β-actin) in BALF from 1 and 2 ppm acute O_3 and filtered air control exposed mice (n =7) * P = 0.025, ** P = 0.009, *** P = 0.0003, **** P <0.0001

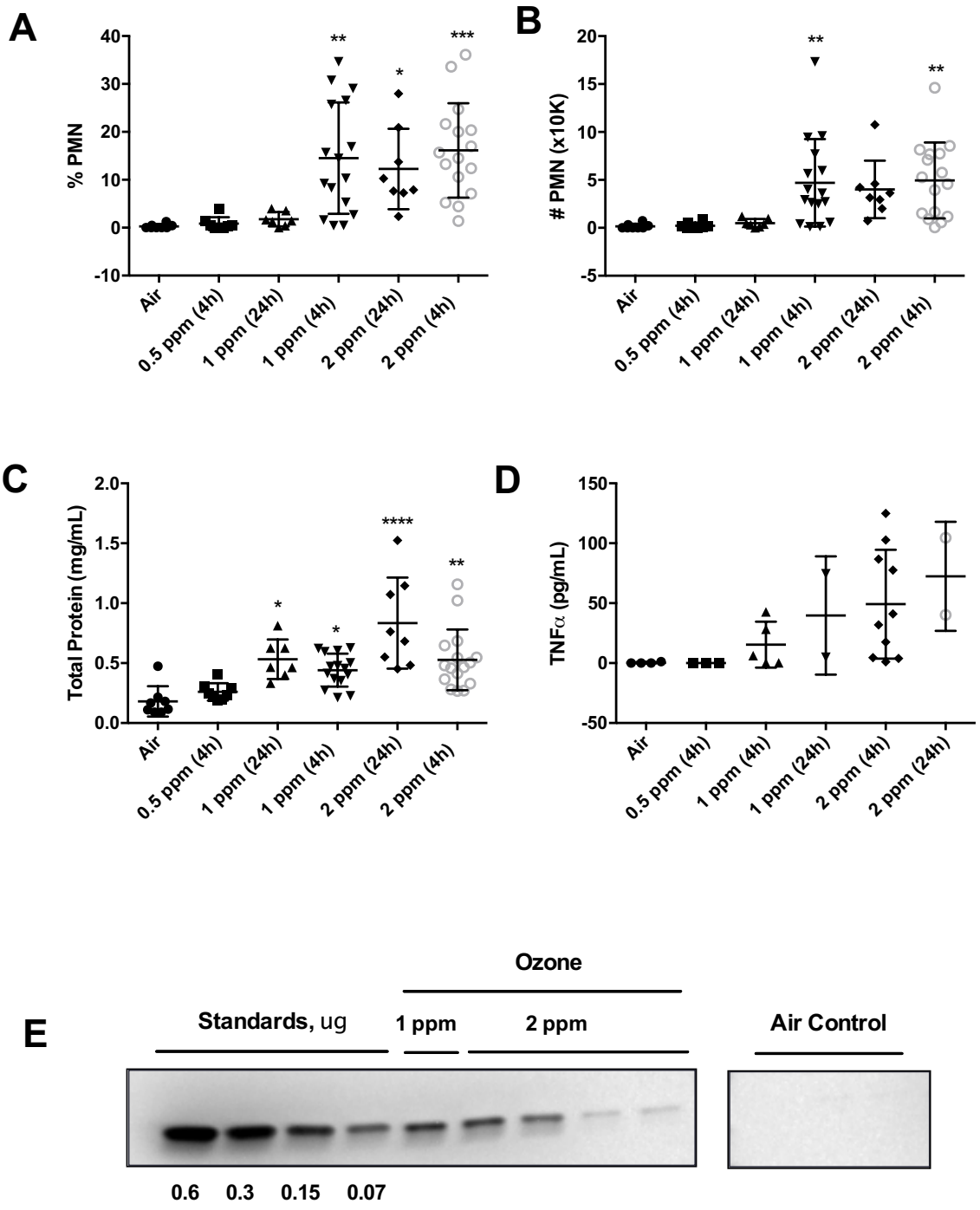

Figure 7 (Continued)

Figure 8. Plasma gelsolin nebulization does not ameliorate ozone-induced lung injury. A: C57BL/6 mice BALF collection 4 h after 2 ppm O_3 exposure (3 h) +/- rhu-pGSN nebulization (30 min) showing % PMN influx, B: total # of PMN (x10K) and C: BALF total protein (mg/mL). D: BALF collection 2 h after the same exposure, showing % PMN influx, E. total PMN # (x10K) and F: BALF total protein (mg/mL), n = 25 G: Western Blot analysis of BALF collected 4 h after 2 ppm O_3 exposure (3 h) +/- rhu-pGSN nebulization showing free actin (42 kDa, β-actin) and (90 kDa, hu-pGSN) (4 μg protein/lane)

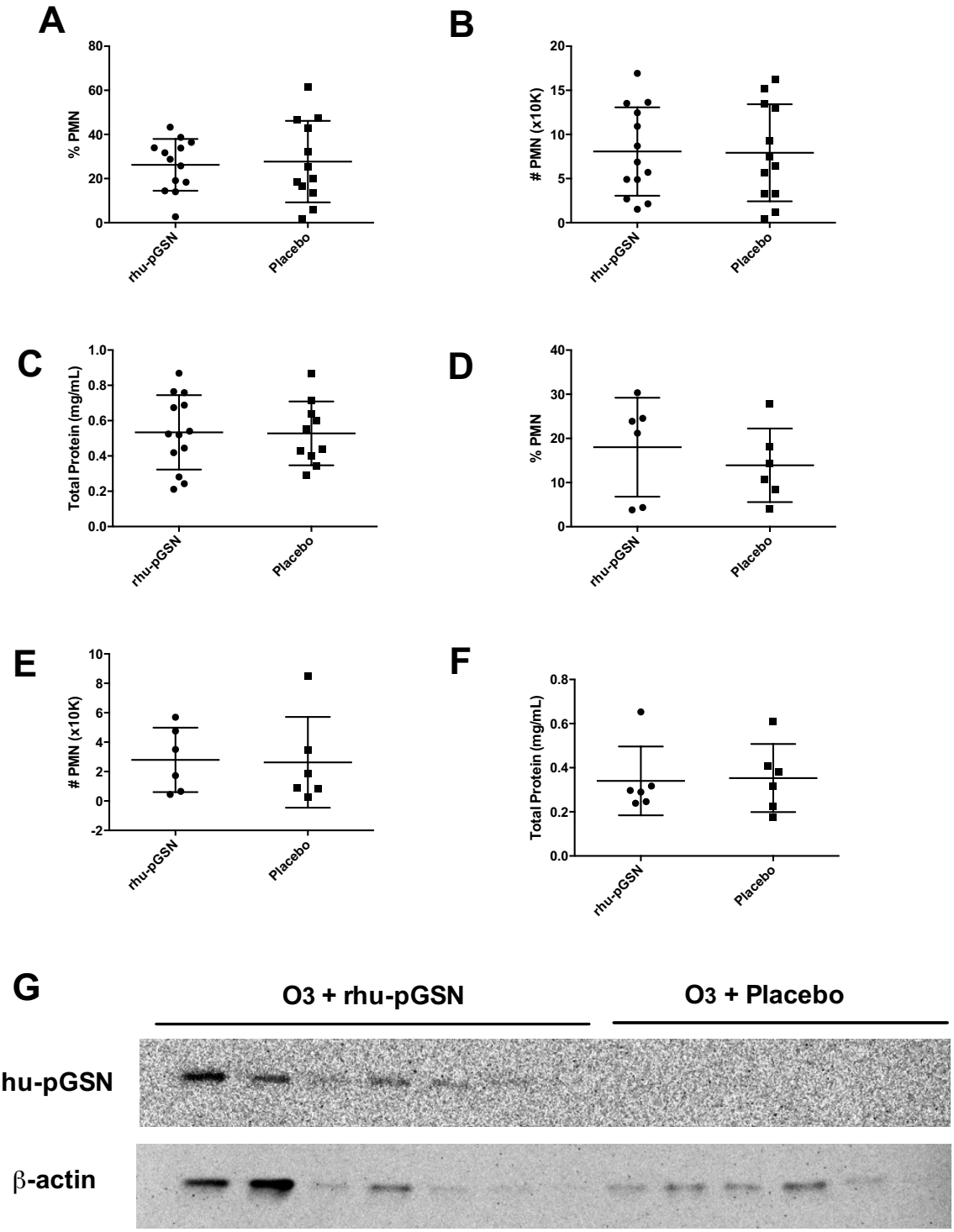

Figure 8 (Continued)

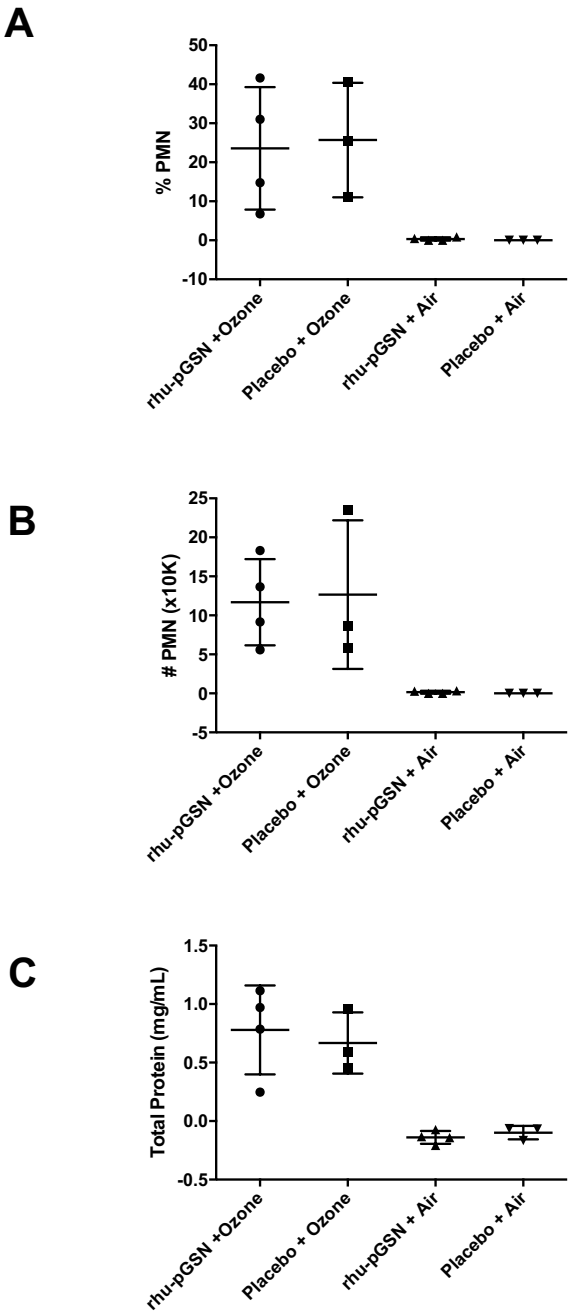

Figure 9. Subcutaneous administration of plasma gelsolin does not ameliorate ozone-induced lung injury. Male C57BL/6 mice pre-treated with rhu-pGSN (11.5mg) or placebo via subcutaneous injection 26 & 2.5 h prior to acute 2 ppm O_3 exposure (3 h), Differential cell counts from BALF collected 4 after O_3 exposure show A: % PMN influx and B: total PMN # (x10K). C: BALF total protein concentration (mg/mL) (n = 14)

Discussion

Acute O_3 exposure resulted in lung injury as observed by free actin release and PMN influx, however varied routes of rhu-pGSN administration did not decrease inflammation, PMN influx and resulting injury as originally predicted. Oxidizing injury is very complex. It is suspected that the neutrophil influx observed in ozone injury is *independent* of actin release, thus accounting for the lack of efficacy of pGSN treatment in addressing PMN levels. Free actin for example does not intrinsically induce PMN influx. C3H/HeJ mice, a TLR4 mutant LPS-resistant model, exhibited no PMN increases in their BAL following intranasal commercial actin instillation (*See Appendix,* Fig. 10). As noted earlier, commercially acquired actin is frequently positive for endotoxin.

Although the independence of PMN influx and actin release in these ozone experiments remains the most likely explanation, it is possible that the route or effective dose of rhu-pGSN administered was insufficient to address the severity of oxidizing injury and PMN influx. Alternatively, even higher levels of resident pGSN, increased with elevated transmucosal barrier permeability due to oxidant damage, may have been sufficient to mask any aid contributed by exogenous pGSN, with ozone injury having failed to exceed the capacity of the extracellular actin-scavenger system (EASS). For example, β-actin levels elevated in the BALF of acute O_3 exposed mice on Western Blotting 4 h following exposure, declined 24 hours later, as pGSN levels appeared to increase slightly over 24 h (*See Appendix,* Fig. 12). It is uncertain however if observed pGSN levels in the BALF represent free, functional protein capable of scavenging actin. Additionally, pGSN depletion so often cited throughout the literature in multiple disease states refers typically to those levels detectable in the circulation, rather than the lung itself. The actions of other compensatory mechanisms or actin binding proteins may further mask the

therapeutic effects of pGSN in O_3-induced lung injury, while the potential benefits of pGSN in non-neutrophilic damage associated with ozone were not assessed. The small amount of variability observed in PMN influx throughout all ozone experiments meanwhile was likely due to mouse variability and O_3 generation and facility fluctuations. Time was not permitting to pursue other in vivo murine lung injury models that might have been more physiologically relevant, controlled and representative of the relationship between actin and pGSN. Our original intent had been to evaluate impaired macrophage bacterial clearance and increased susceptibility in acute O_3 exposed mice to bacterial infection with *S. pneumoniae* followed by amelioration with pGSN. As we were unable to demonstrate measurable benefit of pGSN in O_3-exposed mice in vivo and were satisfied that PMN influx in ozone injury was unrelated to actin release, we proceeded with our detailed evaluation of free actin-mediated macrophage host defense impairment in vitro, as reported in Chapter 1.

Grants

Work reported here was supported by National Institutes of Health Grants HL-7118-40, ES-000002

Thesis Discussion

In the lungs of patients diagnosed with burns and inhalation injury and in murine models of oxidizing injury, influenza infection and secondary pneumococcal postinfluenza infection, we detected free actin release. We next demonstrated impaired alveolar macrophage host defenses in the presence of free actin in vitro. Binding and uptake by a murine lung macrophage derived cell line of *S. pneumoniae*, *S. aureus* and *E. coli* was reduced in the presence of actin, as was primary human alveolar macrophage binding and uptake of fluorescent S. *aureus*. Binding and uptake of *S. pneumoniae* and FL-*S. aureus* was restored with addition of the actin-scavenging protein pGSN. We further demonstrated a mechanism by which extracellular actin may interfere with alveolar macrophage function, through AM binding of free actin by the MARCO scavenger receptor. The release of free actin with subsequent impairment of macrophage host defenses may be highly prevalent in injury and infection, and thus represent a significant therapeutic role for pGSN repletion.

Ozone exposure is linked with increased risk of lung infection, thus we sought to investigate a role for free actin release during oxidizing injury in the lung with subsequent impairment of alveolar macrophage host defenses against bacteria. While we detected free actin in wild type and diabetic murine models of oxidizing injury, varied routes of rhu-pGSN administration failed to aid in reducing O_3-induced PMN influx or transmucosal permeability. Ultimately, oxidizing injuries result in a highly complex, multifaceted injury state. It is believed that the free actin release and PMN influx observed in mice following acute ozone exposure are independent of each other, thus accounting for the lack of pGSN's benefit, at least as measured by neutrophilia.

This hypothesis is further supported by actin's failure to induce PMN influx in vivo as discussed below.

With actin release reported in the injury state, we sought to reproduce injury in the lung through direct actin instillation in vivo. We predicted direct actin instillation would exceed the EASS and resident pGSN levels. Excessive actin filament formation would then lead to lung injury as evidenced by PMN recruitment and increased transmucosal permeability, as measured by increased PMN and total protein in the BALF respectively. We further predicted mice co-instilled with actin and fluorescent latex beads or bacteria would exhibit reduced bead or bacterial binding and uptake, as observed via flow cytometry. Repeated attempts to induce actin-mediated lung injury in mice however proved unsuccessful. Intranasal instillation of graded G-actin monomers was observed to induce polymorphonuclear neutrophil and total protein influx into the lungs of C57BL/6 mice, but was ultimately determined to be due to contaminating endotoxin in commercially acquired actin, rather than the inflammatory properties of actin itself. LPS levels were assessed via colorimetric LAL assay. Endotoxin levels of 1.188 EU/mL in a 0.45mg/mL actin preparation or up to 1EU delivered per mouse were detected. The loss of PMN and total protein influx into the lungs of actin-instilled LPS resistant C3H/HeJ mice, a murine phenotype characterized by a TLR4 mutation, confirmed our concerns (*See Appendix* Fig. 10)

Given our demonstration of impaired macrophage binding and uptake of bacteria in the presence of actin in vitro, we next sought to co-instill actin and fluorescently labeled beads (Invitrogen, Carlsbad, CA) directly into mice in vivo. We hoped to observe reduced bead uptake by resident alveolar macrophages in actin-instilled mice, with reversal by pGSN, upon BAL and

flow cytometry. No difference however was observed in the bead uptake of AMs from mice administered beads with actin, control protein or vehicle, although significant actin levels were attained in the lungs of treated mice as observed via Western Blotting of collected BALF (*See Appendix* Fig. 11). Experiments were repeated and varied, with controlled variable alterations including: anesthetic type administered, actin concentration, instillation volume, instillation number, ordering of actin vs. FL-bead instillation, temperature of instilled material and incubation time prior to lavage. No statistically significant reduction in FL-bead uptake by murine AMs in vivo in the presence of instilled free actin, as observed via flow cytometry following lung lavage, was detected in any of the many repeated experiments. The only statistical difference between AM uptake of FL-beads in the presence or absence of actin occurred when Bead/Buffer or Bead/Actin/Buffer mixtures were first allowed to come to RT or were warmed by hand prior to AM delivery. AMs in this instance took up greater numbers of beads in the presence of actin (*data not shown*) in opposition to our prior extensive in vitro AM binding assays. This distinction is currently attributed to a methodological artifact as opposed to a biological phenomenon. Actin in this case may undergo alteration in the rate or degree of its polymerization, it may serve as a stimulatory opsonin, or as a more viscous and effective vehicle for bead delivery to AMs, thus promoting greater uptake of beads that in the presence of buffer alone. High actin viscosity, required actin dose threshold, proteases within the murine sinus, high levels of resident pGSN and other active actin-binding proteins are presumed to account for our inability to demonstrate actin toxicity within the lung or altered macrophage behavior in vivo. Continuous actin perfusion into the mouse or more direct instillation into the lung may help to exceed these experimental challenges.

Investigation of free actin release and impairment of host defenses in vivo should be pursued in a more physiologically relevant, well characterized murine model, such as that generated by oleic acid-induced lung injury, an acute pulmonary murine injury model characterized by pathology similar to human ARDS (64, 165, 166). Given the difficulties in exceeding the EASS following lung injury and in the reliable induction of free actin release in vivo, pGSN activity within the lung might be monitored differently in future experiments. While pGSN:Actin complexes have long been observed in the circulation following lung injury (64), radiolabelled pGSN administered via subcutaneous injection might travel to the injured lung and be detected in complex with actin in the BALF of treated mice for example. Though somewhat lacking in experimental control, actin-containing BALF transferred from infected or lung-injured mice might also reduce AM binding and uptake of bacteria in vitro, with reversal by pGSN.

Notably, improved delineation of the paths, progression and rate of actin release during injury and infection provides a promising course of study. Is free actin release from dying cells typically more organized, with filaments first carefully exposed on the cell surface for display or is actin shuttled from dying cells contained within budding membranes as extracellular vesicles known as exosomes, or are heavily damaged cells simply split open to spill their actin contents into the extracellular milieu? Furthermore, if actin serves as a DAMP, is the expression and translation of pGSN, its highly conserved scavenging molecule, carefully balanced to control the message, while also removing potentially damaging excess free actin? Perhaps vesicular containment shields free actin from high levels of circulating plasma gelsolin, critical in the event of extreme stress or injury characterized by heavy free actin releases.

The nature of actin release during injury and infection, with subsequent cellular and receptor interactions, and thus ultimately communications, must be further delineated. As noted above, exposed actin filaments on necrotic cells have been recently characterized as a Damage Associated Molecular Pattern or DAMP. Actin was cited as a Clec9a (DNGR-1) receptor ligand (38-40), a DC C-type lectin receptor known to recognize necrotic cells (41). Here we demonstrate free actin binding to AMs and the MARCO scavenger receptor, both prominent innate immune system actors, although a role for actin in adaptive immunity is not precluded. Does actin serve here as a DAMP however, relaying information to AMs concerning cellular and tissue injury and thus stimulating sterile-inflammation, while also impairing macrophage bacterial clearance? It is unknown if other phagocytic immune cells such as PMNs or other resident tissue macrophages bind free actin and also experience bacterial clearance impairment. Different tissue specific isoactins furthermore exist and exhibit different properties (10, 20-22), which may impact their potential roles as receptor ligands. Similarly, although actin-MARCO AM interaction is suspected to be predominantly with filamentous actin, we did not investigate specific distinctions between F and G actin binding properties, different ratios of these species or the effects of varying ionic concentrations.

Notably, while we demonstrated robust MARCO-mediated AM binding of free actin, this did not account for 100% of observed binding. Further characterization of other receptor candidates for binding of exposed free actin, as well as any potential downstream chemokine and cytokine-signaling cascades is of interest. Receptors localized to macrophages, other phagocytes or pulmonary epithelial cells also demonstrating specificity for polyanionic ligands with aggregated conserved patterns associated with cell death, damage or pathogens may all be potential

candidates for actin binding. As was observed experimentally, the class A scavenger receptor SRA-I/II accounted for some actin binding, although redundancy and compensation for the absent MARCO receptor is a suspected factor. The class B macrophage scavenger receptor CD36 is recommended for investigation of potential actin binding. Detected on AMs (167), CD36 has diverse ligands, many of which also interact with Toll Like Receptors (TLRs), and is known to promote sterile inflammation in response to more than one ligand (168). The class A Scavenger Receptor with C-type Lectin (SRCL) type 1, containing a C-type lectin/carbohydrate recognition domain, has high expression in the lung, exhibited *E. coli* and *S. aureus* recognition and binding, and might also be examined further (169, 170), as could the lectin-like oxidized LDL receptor (LOX-1), varied members of the Class II C-type lectin receptors or perhaps the macrophage mannose receptor (MMR) (171). Notably, multiple eukaryotic motility proteins bear similarities to bacterial proteins. Actin and bacterial flagellin may have N-terminal sequence matches (172). TLR5 found on the macrophage surface, recognizes varied flagellin and the actin-binding protein profilin and thus might also serve as a candidate for free actin binding investigation (173, 174). Intracellular TLR11, which exhibits a similar recognition pattern, is not found in humans, but bears resemblance to TLR5 and may be useful in comparable mouse models of disease (173). Many scavenger receptors on macrophages or other cells types, as well as non-scavenger receptors may be discerned to be involved in actin binding, recognition or signaling (175), including cell surface and intracellular TLRs. Potential actin-binding candidates may be discerned through a combination of varied pharmacologic ligand binding assays (176) or via a process of reverse elimination in the assessment of patterns of gene and protein expression among innate signaling transduction pathway cytokines and chemokines. Given endotoxin contamination of commercial actin, LPS resistant C3H/HeJ mice provide a murine model in

which alveolar macrophages may be collected ex vivo and activated with free actin. Subsequent Quantitative PCR, microarray or ELISA testing may reveal differential expression between signaling molecules from actin vs. buffer treated cells. When used in combination with varied inhibitors, anti-MARCO, other antibodies, knockout or knockdown cell lines or murine models it is hoped that other potential actin binding partners and relevant pathways will be elucidated (177). Better characterization of the role of free actin binding by AMs in lung injury and infection will further reveal extracellular actin's significance as a DAMP and its ability to impair AM host defenses, while also expanding the therapeutic repertoire and potential of pGSN.

Appendix:

Methods and Materials

Murine Actin Intranasal Instillation to Induce Lung Injury.

Graded G-actin monomers of rabbit skeletal muscle (Cytoskeleton, Denver, CO) (1-250 μg) in GAB were prepared as above. 8 – 10 week old C57BL/6 mice anesthetized with 120 mg/kg ketamine plus 16 mg/kg xylazine (Vedco, St. Joseph, MO) via intraperitoneal (i.p.) injection received an i.n instillation of 25- or 50-μl of cold actin in suspension (1-250 μg). Mice were sacrificed 24 h later via lethal overdose of i.p. sodium pentobarbital (Fatal-Plus, Vortech Pharmaceuticals, Dearborn, MI). In order to assess the degree of injury in the lung, BAL was performed as above. The proximal trachea of euthanized mice was cannulated and lungs were flushed with 0.6mL of cold phosphate-buffered saline (PBS). The initial lavage fluid was retained, centrifuged cold and separated from BAL cells for later total protein quantitation via colorimetric Bradford Protein Assay (Bio-Rad Laboratories, Hercules, CA (98). Up to 3 mL total BALF in 0.6mL increments were collected per mouse with gentle massage of the thorax. BALF was maintained on ice and centrifuged to separate BAL cells. All cells per mouse were combined and gently resuspended in PBS, counted, and a small fraction underwent cytospin to microscope glass slides for Diff-Quick staining (Baxter Scientific Products) and differential cell count (102). The percentage and total numbers of leukocytes were recorded. As commercial actin is endotoxin positive however, the inflammatory response could be due to LPS (1.188 EU/mL in a 0.45mg/mL actin preparation or as much as 1EU administered per mouse). We thus repeated the procedure in C3H/HeJ mice, an age-matched LPS resistant model with a mutation in TLR4 (Jackson Laboratories) (Bar Harbor, ME).

Murine Actin Intranasal Instillation with Western Blotting Assesses Actin Levels.

As above, 8 – 10 week old mice anesthetized via i.p. injection of ketamine plus xylazine (Vedco, St. Joseph, MO) received an i.n. instillation of 50 μl cold actin suspension (400 μg total). Mice were sacrificed 1 – 1.5 h later via lethal overdose of i.p. sodium pentobarbital (Fatal-Plus, Vortech Pharmaceuticals, Dearborn, MI) for BAL and later Western blotting as above to detect actin.

Murine Actin plus GFP-Bead Co-Instillation.

In this experiment 8 – 10 week old mice received i.p. ketamine plus xylazine (Vedco, St. Joseph, MO) as above, and a 25 μl i.n. instillation of cold actin (50-100 μg), equivalent BSA or buffer, followed 3.5 minutes later by a second instillation of the same plus 12.5 x 10^6 1 μm GFP-latex beads (Invitrogen, Carlsbad, CA). After a 10-minute incubation, mice were sacrificed for BAL. A small portion of sample underwent cytospin for fluorescence microscopy confirming AM uptake of beads, and the remainder was assessed by flow cytometry as before.

Results

Experimental actin-mediated lung injury attributed to endotoxin

As actin is reported in the injury state, we sought to induce lung injury through the direct delivery of actin into mice. Following 1-250 μg actin suspensions via i.n. instillation, BAL was conducted for cytospin, differential cell count and total protein quantitation of BALF. A statistically significant increase in the percentage of polymorphonuclear leukocytes entering the lung was observed with increasing amounts of actin (*Appendix* Fig. 10A). A non-significant trend in increasing total protein influx was also observed (*Appendix* Fig. 10B). When repeated in the LPS resistant C3H/HeJ mouse however, we failed to observe any increase in the number of

PMNs or total protein entering the lung (*Appendix* Fig. 10D-F), thus attributing the initial response to LPS.

Instilled actin fails to impair fluorescent bead uptake by alveolar macrophages in vivo

Actin instilled via the nares of mice was detectable on Western Blotting of BALF collected via lung lavage yet actin levels were well below the quantity instilled (*Appendix* Fig. 11A). Actin levels were insufficient to reduce uptake by resident alveolar macrophages of GFP-labeled 1μm latex beads (Invitrogen) compared to beads co-instilled in mice with control protein or buffer alone as observed via fluorescence microscopy or flow cytometry (*Appendix* Fig. 11B-E).

Figure 10. Intranasal instillation of actin induces lung injury via endotoxin contamination. Graded actin, LPS or vehicle (GAB/H_2O) instilled (i.n.) into mice with BAL 24 h post-treatment A: % PMN in C57BL/6 mice B: Total # PMN (x10K) in C57BL/6, C: BALF total protein (μg/mL) in C57BL/6 (n = 14) D: % PMN in C3H/HeJ mice E: Total # PMN (x10K) in C3H/HeJ F: BALF total protein (μg/mL) in C3H/HeJ (n = 57) * P = 0.03 *** P = 0.0005 **** P <0.0001

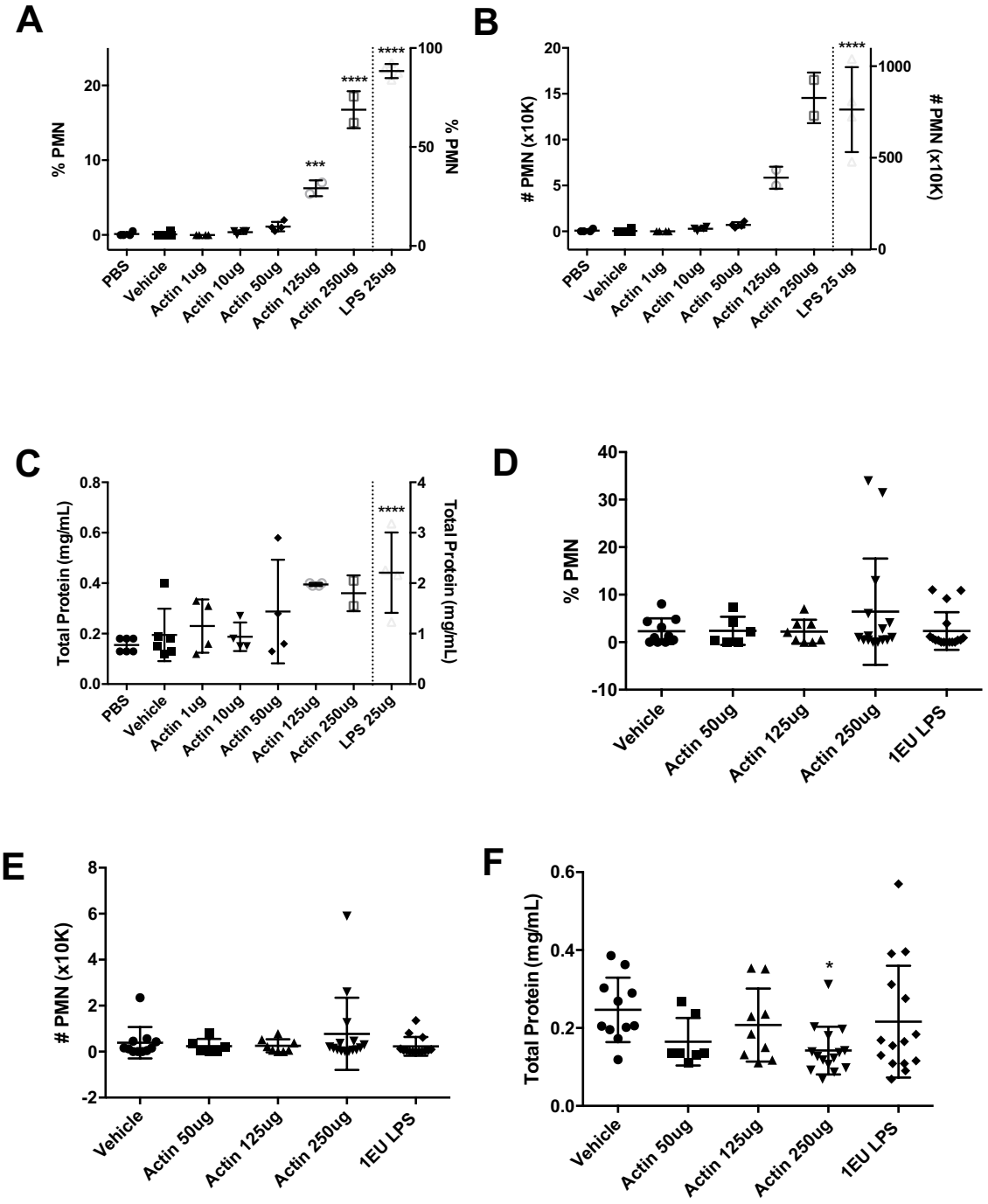

Figure 10 (Continued)

Figure 11. Instilled actin reaches the lung, but fails to impair fluorescent bead uptake by alveolar macrophages. A: 1-1.5 h after 50 μl i.n. actin instillation (400 μg), Western Blot analysis of C57BL/6 mice BAL shows detectable levels of β-actin (45 kDa) compared to actin standard curve (rabbit skeletal muscle actin, μg), 2.5 μg/lane (n = 8) B: Representative image of AM uptake of 1 μm GFP-latex bead via fluorescence microscopy. C: BALF from mouse instilled with 12.5 x 10^6 beads and buffer D: BSA (100 μg) E: or actin (100 μg)

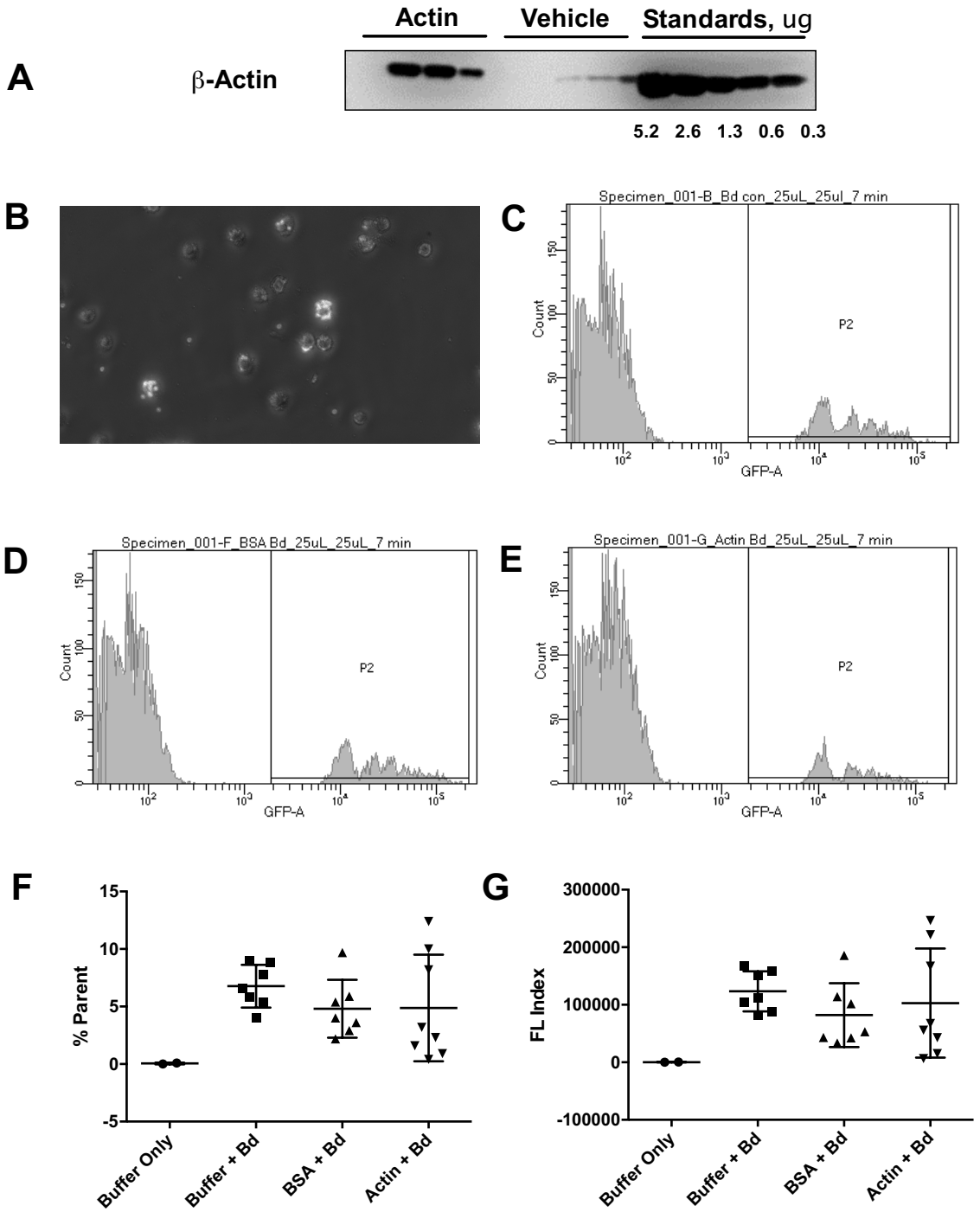

Figure 11 (Continued)

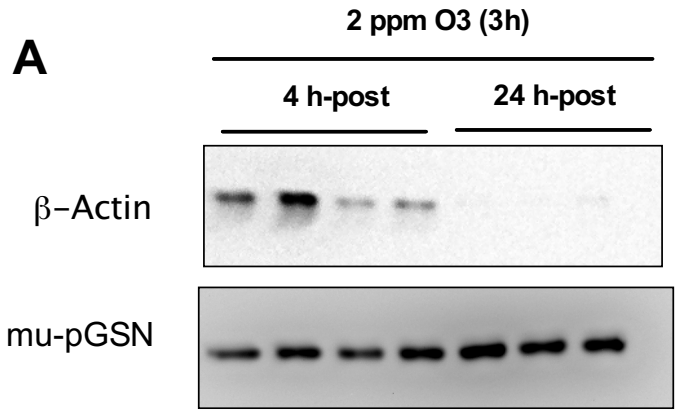

Figure 12. Free actin and pGSN in BALF of ozone exposed mice. BALF collected from male C57BL/6 mice 4 and 24 h after 2 ppm acute O_3 exposure. Western Blot analysis showing free actin (42 kDa, β-actin) at 4 h post exposure, but cleared by 24 h. mu-pGSN (90 kDa) remain unchanged or even increase slightly with acute O_3 exposure (n = 7)

Bibliography

1. Chang DW, Hayashi S, Gharib SA, Vaisar T, King ST, Tsuchiya M, et al. Proteomic and computational analysis of bronchoalveolar proteins during the course of the acute respiratory distress syndrome. Am J Respir Crit Care Med. 2008;178(7):701-9.

2. Haddad JG, Harper KD, Guoth M, Pietra GG, Sanger JW. Angiopathic consequences of saturating the plasma scavenger system for actin. Proceedings of the National Academy of Sciences of the United States of America. 1990;87(4):1381-5.

3. Lee WM, Galbraith RM. The extracellular actin-scavenger system and actin toxicity. The New England journal of medicine. 1992;326(20):1335-41.

4. Lind SE, Smith DB, Janmey PA, Stossel TP. Depression of gelsolin levels and detection of gelsolin-actin complexes in plasma of patients with acute lung injury. Am Rev Respir Dis. 1988;138(2):429-34.

5. Yang Z, Chiou TT, Stossel TP, Kobzik L. Plasma gelsolin improves lung host defense against pneumonia by enhancing macrophage NOS3 function. Am J Physiol Lung Cell Mol Physiol. 2015;309(1):L11-6.

6. Al Ashry HS, Mansour G, Kalil AC, Walters RW, Vivekanandan R. Incidence of ventilator associated pneumonia in burn patients with inhalation injury treated with high frequency percussive ventilation versus volume control ventilation: A systematic review. Burns : journal of the International Society for Burn Injuries. 2016;42(6):1193-200.

7. Dreyfuss D, Ricard JD. Acute lung injury and bacterial infection. Clinics in chest medicine. 2005;26(1):105-12.

8. Shrestha S, Foxman B, Weinberger DM, Steiner C, Viboud C, Rohani P. Identifying the interaction between influenza and pneumococcal pneumonia using incidence data. Sci Transl Med. 2013;5(191):191ra84.

9. Small CL, Shaler CR, McCormick S, Jeyanathan M, Damjanovic D, Brown EG, et al. Influenza infection leads to increased susceptibility to subsequent bacterial superinfection by impairing NK cell responses in the lung. J Immunol. 2010;184(4):2048-56.

10. McHugh KM, Crawford K, Lessard JL. A comprehensive analysis of the developmental and tissue-specific expression of the isoactin multigene family in the rat. Developmental biology. 1991;148(2):442-58.

11. Ankenbauer T, Kleinschmidt JA, Walsh MJ, Weiner OH, Franke WW. Identification of a widespread nuclear actin binding protein. Nature. 1989;342(6251):822-5.

12. Andrin C, McDonald D, Attwood KM, Rodrigue A, Ghosh S, Mirzayans R, et al. A requirement for polymerized actin in DNA double-strand break repair. Nucleus (Austin, Tex). 2012;3(4):384-95.

13. Coutts AS, Weston L, La Thangue NB. A transcription co-factor integrates cell adhesion and motility with the p53 response. Proceedings of the National Academy of Sciences of the United States of America. 2009;106(47):19872-7.

14. Hendzel MJ. The F-act's of nuclear actin. Current opinion in cell biology. 2014;28:84-9.

15. Johnson MA, Sharma M, Mok MT, Henderson BR. Stimulation of in vivo nuclear transport dynamics of actin and its co-factors IQGAP1 and Rac1 in response to DNA replication stress. Biochimica et biophysica acta. 2013;1833(10):2334-47.

16. Weston L, Coutts AS, La Thangue NB. Actin nucleators in the nucleus: an emerging theme. Journal of cell science. 2012;125(Pt 15):3519-27.

17. Tripathi SC. A possible role of actin in the mechanical control of the cell cycle. Biology of the cell. 1989;67(3):351-3.

18. Pollard TD. Actin and Actin-Binding Proteins. Cold Spring Harbor perspectives in biology. 2016;8(8).

19. Huxley HE. ELECTRON MICROSCOPE STUDIES ON THE STRUCTURE OF NATURAL AND SYNTHETIC PROTEIN FILAMENTS FROM STRIATED MUSCLE. Journal of molecular biology. 1963;7:281-308.

20. Vandekerckhove J, Weber K. At least six different actins are expressed in a higher mammal: an analysis based on the amino acid sequence of the amino-terminal tryptic peptide. Journal of molecular biology. 1978;126(4):783-802.

21. Morioka K, Takano-Ohmuro H. Localizations of gamma-Actins in Skin, Hair, Vibrissa, Arrector Pili Muscle and Other Hair Appendages of Developing Rats. Acta histochemica et cytochemica. 2016;49(2):47-65.

22. Bergeron SE, Zhu M, Thiem SM, Friderici KH, Rubenstein PA. Ion-dependent polymerization differences between mammalian beta- and gamma-nonmuscle actin isoforms. The Journal of biological chemistry. 2010;285(21):16087-95.

23. Grinnell F, Baxter CR, Zhu M, Yin HL. Detection of the actin scavenger system in burn wound fluid. Wound repair and regeneration : official publication of the Wound Healing Society [and] the European Tissue Repair Society. 1993;1(4):236-43.

24. Fang JF, Shih LY, Yuan KC, Fang KY, Hwang TL, Hsieh SY. Proteomic analysis of post-hemorrhagic shock mesenteric lymph. Shock (Augusta, Ga). 2010;34(3):291-8.

25. Dzieciatkowska M, Wohlauer MV, Moore EE, Damle S, Peltz E, Campsen J, et al. Proteomic analysis of human mesenteric lymph. Shock (Augusta, Ga). 2011;35(4):331-8.

26. Mittal A, Middleditch M, Ruggiero K, Loveday B, Delahunt B, Jullig M, et al. Changes in the mesenteric lymph proteome induced by hemorrhagic shock. Shock (Augusta, Ga). 2010;34(2):140-9.

27. Lee WM, Reines D, Watt GH, Cook JA, Wise WC, Halushka PV, et al. Alterations in Gc levels and complexing in septic shock. Circulatory shock. 1989;28(3):249-55.

28. Goldschmidt-Clermont PJ, Lee WM, Galbraith RM. Proportion of circulating Gc (vitamin D-binding protein) in complexed form: relation to clinical outcome in fulminant hepatic necrosis. Gastroenterology. 1988;94(6):1454-8.

29. Lee WM, Emerson DL, Werner PA, Arnaud P, Goldschmidt-Clermont P, Galbraith RM. Decreased serum group-specific component protein levels and complexes with actin in fulminant hepatic necrosis. Hepatology (Baltimore, Md). 1985;5(2):271-5.

30. Emerson DL, Arnaud P, Galbraith RM. Evidence of increased Gc:actin complexes in pregnant serum: a possible result of trophoblast embolism. Am J Reprod Immunol. 1983;4(4):185-9.

31. Smith DB, Janmey PA, Sherwood JA, Howard RJ, Lind SE. Decreased plasma gelsolin levels in patients with Plasmodium falciparum malaria: a consequence of hemolysis? Blood. 1988;72(1):214-8.

32. Erukhimov JA, Tang ZL, Johnson BA, Donahoe MP, Razzack JA, Gibson KF, et al. Actin-containing sera from patients with adult respiratory distress syndrome are toxic to sheep pulmonary endothelial cells. Am J Respir Crit Care Med. 2000;162(1):288-94.

33. Bhargava M, Higgins L, Wendt CH, Ingbar DH. Application of clinical proteomics in acute respiratory distress syndrome. Clinical and translational medicine. 2014;3(1):34.

34. Nguyen EV, Gharib SA, Palazzo SJ, Chow YH, Goodlett DR, Schnapp LM. Proteomic profiling of bronchoalveolar lavage fluid in critically ill patients with ventilator-associated pneumonia. PLoS One. 2013;8(3):e58782.

35. Mejean C, Roustan C, Benyamin Y. Anti-actin antibodies. Detection and quantitation of total and skeletal muscle actin in human plasma using a competitive ELISA. J Immunol Methods. 1987;99(1):129-35.

36. Gabbiani G, Ryan GB, Lamelin JP, Vassalli P, Majno G, Bouvier CA, et al. Human smooth muscle autoantibody. Its identification as antiactin antibody and a study of its binding to "nonmuscular" cells. Am J Pathol. 1973;72(3):473-88.

37. Frenzel C, Herkel J, Luth S, Galle PR, Schramm C, Lohse AW. Evaluation of F-actin ELISA for the diagnosis of autoimmune hepatitis. The American journal of gastroenterology. 2006;101(12):2731-6.

38. Ahrens S, Zelenay S, Sancho D, Hanc P, Kjaer S, Feest C, et al. F-actin is an evolutionarily conserved damage-associated molecular pattern recognized by DNGR-1, a receptor for dead cells. Immunity. 2012;36(4):635-45.

39. Geijtenbeek TB. Actin' as a death signal. Immunity. 2012;36(4):557-9.

40. Zhang JG, Czabotar PE, Policheni AN, Caminschi I, Wan SS, Kitsoulis S, et al. The dendritic cell receptor Clec9A binds damaged cells via exposed actin filaments. Immunity. 2012;36(4):646-57.

41. Sancho D, Joffre OP, Keller AM, Rogers NC, Martinez D, Hernanz-Falcon P, et al. Identification of a dendritic cell receptor that couples sensing of necrosis to immunity. Nature. 2009;458(7240):899-903.

42. Janmey PA, Lamb JA, Ezzell RM, Hvidt S, Lind SE. Effects of actin filaments on fibrin clot structure and lysis. Blood. 1992;80(4):928-36.

43. Janmey PA, Lind SE, Yin HL, Stossel TP. Effects of semi-dilute actin solutions on the mobility of fibrin protofibrils during clot formation. Biochimica et biophysica acta. 1985;841(2):151-8.

44. Scarborough VD, Bradford HR, Ganguly P. Aggregation of platelets by muscle actin. A multivalent interaction model of platelet aggregation by ADP. Biochemical and biophysical research communications. 1981;100(3):1314-9.

45. Wettero J, Askendal A, Tengvall P, Bengtsson T. Interactions between surface-bound actin and complement, platelets, and neutrophils. Journal of biomedical materials research Part A. 2003;66(1):162-75.

46. Thuijls G, de Haan JJ, Derikx JP, Daissormont I, Hadfoune M, Heineman E, et al. Intestinal cytoskeleton degradation precedes tight junction loss following hemorrhagic shock. Shock (Augusta, Ga). 2009;31(2):164-9.

47. Lee PS, Patel SR, Christiani DC, Bajwa E, Stossel TP, Waxman AB. Plasma gelsolin depletion and circulating actin in sepsis: a pilot study. PLoS One. 2008;3(11):e3712.

48. Osborn TM, Verdrengh M, Stossel TP, Tarkowski A, Bokarewa M. Decreased levels of the gelsolin plasma isoform in patients with rheumatoid arthritis. Arthritis research & therapy. 2008;10(5):R117.

49. Dahl B, Schiodt FV, Ott P, Gvozdenovic R, Yin HL, Lee WM. Plasma gelsolin is reduced in trauma patients. Shock (Augusta, Ga). 1999;12(2):102-4.

50. Huang S, Rhoads SL, DiNubile MJ. Temporal association between serum gelsolin levels and clinical events in a patient with severe falciparum malaria. Clinical infectious diseases : an official publication of the Infectious Diseases Society of America. 1997;24(5):951-4.

51. DiNubile MJ, Stossel TP, Ljunghusen OC, Ferrara JL, Antin JH. Prognostic implications of declining plasma gelsolin levels after allogeneic stem cell transplantation. Blood. 2002;100(13):4367-71.

52. DiNubile MJ. Plasma gelsolin levels in the diagnosis, prognosis, and treatment of lung complications of prematurity. Am J Respir Crit Care Med. 2012;186(11):1195-6.

53. Yin HL, Stossel TP. Control of cytoplasmic actin gel-sol transformation by gelsolin, a calcium-dependent regulatory protein. Nature. 1979;281(5732):583-6.

54. Yin HL, Kwiatkowski DJ, Mole JE, Cole FS. Structure and biosynthesis of cytoplasmic and secreted variants of gelsolin. The Journal of biological chemistry. 1984;259(8):5271-6.

55. Kwiatkowski DJ, Mehl R, Yin HL. Genomic organization and biosynthesis of secreted and cytoplasmic forms of gelsolin. The Journal of cell biology. 1988;106(2):375-84.

56. Kwiatkowski DJ, Stossel TP, Orkin SH, Mole JE, Colten HR, Yin HL. Plasma and cytoplasmic gelsolins are encoded by a single gene and contain a duplicated actin-binding domain. Nature. 1986;323(6087):455-8.

57. Kwiatkowski DJ, Mehl R, Izumo S, Nadal-Ginard B, Yin HL. Muscle is the major source of plasma gelsolin. The Journal of biological chemistry. 1988;263(17):8239-43.

58. Smith DB, Janmey PA, Herbert TJ, Lind SE. Quantitative measurement of plasma gelsolin and its incorporation into fibrin clots. The Journal of laboratory and clinical medicine. 1987;110(2):189-95.

59. Bryan J, Kurth MC. Actin-gelsolin interactions. Evidence for two actin-binding sites. The Journal of biological chemistry. 1984;259(12):7480-7.

60. Yin HL, Iida K, Janmey PA. Identification of a polyphosphoinositide-modulated domain in gelsolin which binds to the sides of actin filaments. The Journal of cell biology. 1988;106(3):805-12.

61. Yin HL, Zaner KS, Stossel TP. Ca2+ control of actin gelation. Interaction of gelsolin with actin filaments and regulation of actin gelation. The Journal of biological chemistry. 1980;255(19):9494-500.

62. Janmey PA, Iida K, Yin HL, Stossel TP. Polyphosphoinositide micelles and polyphosphoinositide-containing vesicles dissociate endogenous gelsolin-actin complexes and promote actin assembly from the fast-growing end of actin filaments blocked by gelsolin. The Journal of biological chemistry. 1987;262(25):12228-36.

63. McGough AM, Staiger CJ, Min JK, Simonetti KD. The gelsolin family of actin regulatory proteins: modular structures, versatile functions. FEBS letters. 2003;552(2-3):75-81.

64. Smith DB, Janmey PA, Lind SE. Circulating actin-gelsolin complexes following oleic acid-induced lung injury. Am J Pathol. 1988;130(2):261-7.

65. Janmey PA, Stossel TP, Lind SE. Sequential binding of actin monomers to plasma gelsolin and its inhibition by vitamin D-binding protein. Biochemical and biophysical research communications. 1986;136(1):72-9.

66. Haddad JG, Jr. Transport of vitamin D metabolites. Clinical orthopaedics and related research. 1979(142):249-61.

67. Goldschmidt-Clermont PJ, Galbraith RM, Emerson DL, Marsot F, Nel AE, Arnaud P. Distinct sites on the G-actin molecule bind group-specific component and deoxyribonuclease I. The Biochemical journal. 1985;228(2):471-7.

68. Van Baelen H, Bouillon R, De Moor P. Vitamin D-binding protein (Gc-globulin) binds actin. The Journal of biological chemistry. 1980;255(6):2270-2.

69. Daiger SP, Schanfield MS, Cavalli-Sforza LL. Group-specific component (Gc) proteins bind vitamin D and 25-hydroxyvitamin D. Proceedings of the National Academy of Sciences of the United States of America. 1975;72(6):2076-80.

70. Cooke NE, Haddad JG. Vitamin D binding protein (Gc-globulin). Endocrine reviews. 1989;10(3):294-307.

71. Dueland S, Nenseter MS, Drevon CA. Uptake and degradation of filamentous actin and vitamin D-binding protein in the rat. The Biochemical journal. 1991;274 (Pt 1):237-41.

72. Goldschmidt-Clermont PJ, Van Baelen H, Bouillon R, Shook TE, Williams MH, Nel AE, et al. Role of group-specific component (vitamin D binding protein) in clearance of actin from the circulation in the rabbit. J Clin Invest. 1988;81(5):1519-27.

73. Lind SE, Smith DB, Janmey PA, Stossel TP. Role of plasma gelsolin and the vitamin D-binding protein in clearing actin from the circulation. J Clin Invest. 1986;78(3):736-42.

74. Chien YW, Klugman KP, Morens DM. Bacterial pathogens and death during the 1918 influenza pandemic. The New England journal of medicine. 2009;361(26):2582-3.

75. Klugman KP, Chien YW, Madhi SA. Pneumococcal pneumonia and influenza: a deadly combination. Vaccine. 2009;27 Suppl 3:C9-c14.

76. Lindsay MI, Jr., Herrmann EC, Jr., Morrow GW, Jr., Brown AL, Jr. Hong Kong influenza: clinical, microbiologic, and pathologic features in 127 cases. Jama. 1970;214(10):1825-32.

77. McCullers JA, English BK. Improving therapeutic strategies for secondary bacterial pneumonia following influenza. Future microbiology. 2008;3(4):397-404.

78. Morens DM, Fauci AS. The 1918 influenza pandemic: insights for the 21st century. J Infect Dis. 2007;195(7):1018-28.

79. Morens DM, Taubenberger JK, Fauci AS. Predominant role of bacterial pneumonia as a cause of death in pandemic influenza: implications for pandemic influenza preparedness. J Infect Dis. 2008;198(7):962-70.

80. Trotter Y, Jr., Dunn FL, Drachman RH, Henderson DA, Pizzi M, Langmuir AD. Asian influenza in the United States, 1957-1958. American journal of hygiene. 1959;70(1):34-50.

81. McCullers JA. Insights into the interaction between influenza virus and pneumococcus. Clinical microbiology reviews. 2006;19(3):571-82.

82. Ballinger MN, Standiford TJ. Postinfluenza Bacterial Pneumonia: Host Defenses Gone Awry. Journal of Interferon & Cytokine Research. 2010;30(9):643-52.

83. Rynda-Apple A, Robinson KM, Alcorn JF. Influenza and Bacterial Superinfection: Illuminating the Immunologic Mechanisms of Disease. Infect Immun. 2015;83(10):3764-70.

84. Plotkowski MC, Puchelle E, Beck G, Jacquot J, Hannoun C. Adherence of type I Streptococcus pneumoniae to tracheal epithelium of mice infected with influenza A/PR8 virus. Am Rev Respir Dis. 1986;134(5):1040-4.

85. Ramphal R, Fischlschweiger W, Shands JW, Jr., Small PA, Jr. Murine influenzal tracheitis: a model for the study of influenza and tracheal epithelial repair. Am Rev Respir Dis. 1979;120(6):1313-24.

86. Pittet LA, Hall-Stoodley L, Rutkowski MR, Harmsen AG. Influenza virus infection decreases tracheal mucociliary velocity and clearance of Streptococcus pneumoniae. Am J Respir Cell Mol Biol. 2010;42(4):450-60.

87. Hashimoto Y, Moki T, Takizawa T, Shiratsuchi A, Nakanishi Y. Evidence for phagocytosis of influenza virus-infected, apoptotic cells by neutrophils and macrophages in mice. J Immunol. 2007;178(4):2448-57.

88. Herold S, Steinmueller M, von Wulffen W, Cakarova L, Pinto R, Pleschka S, et al. Lung epithelial apoptosis in influenza virus pneumonia: the role of macrophage-expressed TNF-related apoptosis-inducing ligand. J Exp Med. 2008;205(13):3065-77.

89. Sun K, Metzger DW. Inhibition of pulmonary antibacterial defense by interferon-gamma during recovery from influenza infection. Nature medicine. 2008;14(5):558-64.

90. LeVine AM, Koeningsknecht V, Stark JM. Decreased pulmonary clearance of S. pneumoniae following influenza A infection in mice. Journal of virological methods. 2001;94(1-2):173-86.

91. Shahangian A, Chow EK, Tian X, Kang JR, Ghaffari A, Liu SY, et al. Type I IFNs mediate development of postinfluenza bacterial pneumonia in mice. J Clin Invest. 2009;119(7):1910-20.

92. Vasconcellos CA, Allen PG, Wohl ME, Drazen JM, Janmey PA, Stossel TP. Reduction in viscosity of cystic fibrosis sputum in vitro by gelsolin. Science (New York, NY). 1994;263(5149):969-71.

93. Hocking WG, Golde DW. The pulmonary-alveolar macrophage (first of two parts). The New England journal of medicine. 1979;301(11):580-7.

94. Hocking WG, Golde DW. The pulmonary-alveolar macrophage (second of two parts). The New England journal of medicine. 1979;301(12):639-45.

95. Twigg HL, 3rd. Macrophages in innate and acquired immunity. Seminars in respiratory and critical care medicine. 2004;25(1):21-31.

96. Arredouani M, Yang Z, Ning Y, Qin G, Soininen R, Tryggvason K, et al. The scavenger receptor MARCO is required for lung defense against pneumococcal pneumonia and inhaled particles. J Exp Med. 2004;200(2):267-72.

97. Shore SA, Rivera-Sanchez YM, Schwartzman IN, Johnston RA. Responses to ozone are increased in obese mice. J Appl Physiol (1985). 2003;95(3):938-45.

98. Yang Z, Huang YC, Koziel H, de Crom R, Ruetten H, Wohlfart P, et al. Female resistance to pneumonia identifies lung macrophage nitric oxide synthase-3 as a therapeutic target. eLife. 2014;3.

99. Maile R, Jones S, Pan Y, Zhou H, Jaspers I, Peden DB, et al. Association between early airway damage-associated molecular patterns and subsequent bacterial infection in patients with inhalational and burn injury. Am J Physiol Lung Cell Mol Physiol. 2015;308(9):L855-60.

100. Lee PS, Waxman AB, Cotich KL, Chung SW, Perrella MA, Stossel TP. Plasma gelsolin is a marker and therapeutic agent in animal sepsis. Critical care medicine. 2007;35(3):849-55.

101. Gonzalez E, Kou R, Lin AJ, Golan DE, Michel T. Subcellular targeting and agonist-induced site-specific phosphorylation of endothelial nitric-oxide synthase. The Journal of biological chemistry. 2002;277(42):39554-60.

102. Zhou H, Imrich A, Kobzik L. Characterization of immortalized MARCO and SR-AI/II-deficient murine alveolar macrophage cell lines. Part Fibre Toxicol. 2008;5:7.

103. Sulahian TH, Imrich A, Deloid G, Winkler AR, Kobzik L. Signaling pathways required for macrophage scavenger receptor-mediated phagocytosis: analysis by scanning cytometry. Respir Res. 2008;9:59.

104. DeLoid GM, Sulahian TH, Imrich A, Kobzik L. Heterogeneity in macrophage phagocytosis of Staphylococcus aureus strains: high-throughput scanning cytometry-based analysis. PLoS One. 2009;4(7):e6209.

105. Cohen TS, Bucki R, Byfield FJ, Ciccarelli NJ, Rosenberg B, DiNubile MJ, et al. Therapeutic potential of plasma gelsolin administration in a rat model of sepsis. Cytokine. 2011;54(3):235-8.

106. Wai Ming C, Lee Sung L, Keen Man K, Wai Lun L, James CMH, Kin Man C, et al. A Randomized, Double-Blind, Placebo-Controlled, Ascending-Dose Trial Of The Pharmacokinetics And Safety Of Intravenous Infusion Of Recombinant Human Plasma Gelsolin In Acutely Ill Patients With Decreased Plasma Gelsolin Levels. D17 TREATMENTS FOR SEPSIS: ANYTHING NEW? American Thoracic Society International Conference Abstracts: American Thoracic Society; 2011. p. A5601-A.

107. Al-Hegelan M, Tighe RM, Castillo C, Hollingsworth JW. Ambient ozone and pulmonary innate immunity. Immunologic research. 2011;49(1-3):173-91.

108. Bell ML, Dominici F, Samet JM. A meta-analysis of time-series studies of ozone and mortality with comparison to the national morbidity, mortality, and air pollution study. Epidemiology (Cambridge, Mass). 2005;16(4):436-45.

109. Gryparis A, Forsberg B, Katsouyanni K, Analitis A, Touloumi G, Schwartz J, et al. Acute effects of ozone on mortality from the "air pollution and health: a European approach" project. Am J Respir Crit Care Med. 2004;170(10):1080-7.

110. Koren HS. Associations between criteria air pollutants and asthma. Environ Health Perspect. 1995;103 Suppl 6:235-42.

111. Samet JM, Zeger SL, Dominici F, Curriero F, Coursac I, Dockery DW, et al. The National Morbidity, Mortality, and Air Pollution Study. Part II: Morbidity and mortality from air pollution in the United States. Res Rep Health Eff Inst. 2000;94(Pt 2):5-70; discussion 1-9.

112. Chameides WL, Kasibhatla PS, Yienger J, Levy H, 2nd. Growth of continental-scale metro-agro-plexes, regional ozone pollution, and world food production. Science (New York, NY). 1994;264(5155):74-7.

113. Finlayson-Pitts BJ, Pitts JN, Jr. Tropospheric air pollution: ozone, airborne toxics, polycyclic aromatic hydrocarbons, and particles. Science (New York, NY). 1997;276(5315):1045-52.

114. Logan JA. Tropospheric ozone: Seasonal behavior, trends, and anthropogenic influence. Journal of Geophysical Research: Atmospheres. 1985;90(D6):10463-82.

115. Sarzynski A. Bigger Is Not Always Better: A Comparative Analysis of Cities and their Air Pollution Impact. Urban Studies. 2012;49(14):3121-38.

116. Liao H, Chen W-T, Seinfeld JH. Role of climate change in global predictions of future tropospheric ozone and aerosols. Journal of Geophysical Research: Atmospheres. 2006;111(D12):n/a-n/a.

117. Murazaki K, Hess P. How does climate change contribute to surface ozone change over the United States? Journal of Geophysical Research: Atmospheres. 2006;111(D5):n/a-n/a.

118. Papiez MR, Potosnak MJ, Goliff WS, Guenther AB, Matsunaga SN, Stockwell WR. The impacts of reactive terpene emissions from plants on air quality in Las Vegas, Nevada. Atmospheric Environment. 2009;43(27):4109-23.

119. Pun BK, Wu SY, Seigneur C. Contribution of biogenic emissions to the formation of ozone and particulate matter in the eastern United States. Environmental science & technology. 2002;36(16):3586-96.

120. Akimoto H. Global air quality and pollution. Science (New York, NY). 2003;302(5651):1716-9.

121. West JJ, Fiore AM, Horowitz LW, Mauzerall DL. Global health benefits of mitigating ozone pollution with methane emission controls. Proceedings of the National Academy of Sciences of the United States of America. 2006;103(11):3988-93.

122. Schwartz J. Air pollution and daily mortality: a review and meta analysis. Environmental research. 1994;64(1):36-52.

123. Schwartz J. What are people dying of on high air pollution days? Environmental research. 1994;64(1):26-35.

124. Vagaggini B, Carnevali S, Macchioni P, Taccola M, Fornai E, Bacci E, et al. Airway inflammatory response to ozone in subjects with different asthma severity. Eur Respir J. 1999;13(2):274-80.

125. Alexeeff SE, Litonjua AA, Suh H, Sparrow D, Vokonas PS, Schwartz J. Ozone exposure and lung function: effect modified by obesity and airways hyperresponsiveness in the VA normative aging study. Chest. 2007;132(6):1890-7.

126. Alexis NE, Lay JC, Hazucha M, Harris B, Hernandez ML, Bromberg PA, et al. Low-level ozone exposure induces airways inflammation and modifies cell surface phenotypes in healthy humans. Inhal Toxicol. 2010;22(7):593-600.

127. Folinsbee LJ, McDonnell WF, Horstman DH. Pulmonary function and symptom responses after 6.6-hour exposure to 0.12 ppm ozone with moderate exercise. Japca. 1988;38(1):28-35.

128. Jorres RA, Holz O, Zachgo W, Timm P, Koschyk S, Muller B, et al. The effect of repeated ozone exposures on inflammatory markers in bronchoalveolar lavage fluid and mucosal biopsies. Am J Respir Crit Care Med. 2000;161(6):1855-61.

129. Kim CS, Alexis NE, Rappold AG, Kehrl H, Hazucha MJ, Lay JC, et al. Lung function and inflammatory responses in healthy young adults exposed to 0.06 ppm ozone for 6.6 hours. Am J Respir Crit Care Med. 2011;183(9):1215-21.

130. Medina-Ramon M, Zanobetti A, Schwartz J. The effect of ozone and PM10 on hospital admissions for pneumonia and chronic obstructive pulmonary disease: a national multicity study. American journal of epidemiology. 2006;163(6):579-88.

131. Desqueyroux H, Pujet JC, Prosper M, Le Moullec Y, Momas I. Effects of air pollution on adults with chronic obstructive pulmonary disease. Archives of environmental health. 2002;57(6):554-60.

132. Fauroux B, Sampil M, Quenel P, Lemoullec Y. Ozone: a trigger for hospital pediatric asthma emergency room visits. Pediatric pulmonology. 2000;30(1):41-6.

133. Olsson D, Mogren I, Forsberg B. Air pollution exposure in early pregnancy and adverse pregnancy outcomes: a register-based cohort study. BMJ open. 2013;3(2).

134. Devlin RB, McDonnell WF, Mann R, Becker S, House DE, Schreinemachers D, et al. Exposure of humans to ambient levels of ozone for 6.6 hours causes cellular and biochemical changes in the lung. Am J Respir Cell Mol Biol. 1991;4(1):72-81.

135. Schelegle ES, Siefkin AD, McDonald RJ. Time course of ozone-induced neutrophilia in normal humans. Am Rev Respir Dis. 1991;143(6):1353-8.

136. Bhalla DK, Crocker TT. Pulmonary epithelial permeability in rats exposed to O3. Journal of toxicology and environmental health. 1987;21(1-2):73-87.

137. Bhalla DK, Mannix RC, Kleinman MT, Crocker TT. Relative permeability of nasal, tracheal, and bronchoalveolar mucosa to macromolecules in rats exposed to ozone. Journal of toxicology and environmental health. 1986;17(2-3):269-83.

138. Kleeberger SR, Hudak BB. Acute ozone-induced change in airway permeability: role of infiltrating leukocytes. J Appl Physiol (1985). 1992;72(2):670-6.

139. Kleeberger SR, Seiden JE, Levitt RC, Zhang LY. Mast cells modulate acute ozone-induced inflammation of the murine lung. Am Rev Respir Dis. 1993;148(5):1284-91.

140. Noviski N, Brewer JP, Skornik WA, Galli SJ, Drazen JM, Martin TR. Mast cell activation is not required for induction of airway hyperresponsiveness by ozone in mice. J Appl Physiol (1985). 1999;86(1):202-10.

141. Triantaphyllopoulos K, Hussain F, Pinart M, Zhang M, Li F, Adcock I, et al. A model of chronic inflammation and pulmonary emphysema after multiple ozone exposures in mice. Am J Physiol Lung Cell Mol Physiol. 2011;300(5):L691-700.

142. Bhalla DK. Ozone-induced lung inflammation and mucosal barrier disruption: toxicology, mechanisms, and implications. Journal of toxicology and environmental health Part B, Critical reviews. 1999;2(1):31-86.

143. Mustafa MG. Biochemical basis of ozone toxicity. Free Radic Biol Med. 1990;9(3):245-65.

144. McKinnon KP, Madden MC, Noah TL, Devlin RB. In vitro ozone exposure increases release of arachidonic acid products from a human bronchial epithelial cell line. Toxicol Appl Pharmacol. 1993;118(2):215-23.

145. Shore SA, Johnston RA, Schwartzman IN, Chism D, Krishna Murthy GG. Ozone-induced airway hyperresponsiveness is reduced in immature mice. J Appl Physiol (1985). 2002;92(3):1019-28.

146. Zhao Q, Simpson LG, Driscoll KE, Leikauf GD. Chemokine regulation of ozone-induced neutrophil and monocyte inflammation. Am J Physiol. 1998;274(1 Pt 1):L39-46.

147. Bhalla DK, Rasmussen RE, Daniels DS. Adhesion and motility of polymorphonuclear leukocytes isolated from the blood of rats exposed to ozone: potential biomarkers of toxicity. Toxicol Appl Pharmacol. 1993;123(2):177-86.

148. Garantziotis S, Li Z, Potts EN, Lindsey JY, Stober VP, Polosukhin VV, et al. TLR4 is necessary for hyaluronan-mediated airway hyperresponsiveness after ozone inhalation. Am J Respir Crit Care Med. 2010;181(7):666-75.

149. Dahl M, Bauer AK, Arredouani M, Soininen R, Tryggvason K, Kleeberger SR, et al. Protection against inhaled oxidants through scavenging of oxidized lipids by macrophage receptors MARCO and SR-AI/II. J Clin Invest. 2007;117(3):757-64.

150. Sunil VR, Patel-Vayas K, Shen J, Laskin JD, Laskin DL. Classical and alternative macrophage activation in the lung following ozone-induced oxidative stress. Toxicol Appl Pharmacol. 2012;263(2):195-202.

151. Cho HY, Morgan DL, Bauer AK, Kleeberger SR. Signal transduction pathways of tumor necrosis factor--mediated lung injury induced by ozone in mice. Am J Respir Crit Care Med. 2007;175(8):829-39.

152. Cho HY, Zhang LY, Kleeberger SR. Ozone-induced lung inflammation and hyperreactivity are mediated via tumor necrosis factor-alpha receptors. Am J Physiol Lung Cell Mol Physiol. 2001;280(3):L537-46.

153. Connor AJ, Laskin JD, Laskin DL. Ozone-induced lung injury and sterile inflammation. Role of toll-like receptor 4. Experimental and molecular pathology. 2012;92(2):229-35.

154. Laskin DL, Sunil VR, Gardner CR, Laskin JD. Macrophages and tissue injury: agents of defense or destruction? Annual review of pharmacology and toxicology. 2011;51:267-88.

155. Barry BE, Mercer RR, Miller FJ, Crapo JD. Effects of inhalation of 0.25 ppm ozone on the terminal bronchioles of juvenile and adult rats. Exp Lung Res. 1988;14(2):225-45.

156. Pino MV, Levin JR, Stovall MY, Hyde DM. Pulmonary inflammation and epithelial injury in response to acute ozone exposure in the rat. Toxicol Appl Pharmacol. 1992;112(1):64-72.

157. Coffin DL, Gardner DE. Interaction of biological agents and chemical air pollutants. The Annals of occupational hygiene. 1972;15(2):219-35.

158. Gilmour MI, Park P, Doerfler D, Selgrade MK. Factors that influence the suppression of pulmonary antibacterial defenses in mice exposed to ozone. Exp Lung Res. 1993;19(3):299-314.

159. Allegra L, Moavero NE, Rampoldi C. Ozone-induced impairment of mucociliary transport and its prevention with N-acetylcysteine. The American journal of medicine. 1991;91(3c):67s-71s.

160. Foster WM, Costa DL, Langenback EG. Ozone exposure alters tracheobronchial mucociliary function in humans. J Appl Physiol (1985). 1987;63(3):996-1002.

161. Karavitis J, Kovacs EJ. Macrophage phagocytosis: effects of environmental pollutants, alcohol, cigarette smoke, and other external factors. J Leukoc Biol. 2011;90(6):1065-78.

162. Mikerov AN, Umstead TM, Gan X, Huang W, Guo X, Wang G, et al. Impact of ozone exposure on the phagocytic activity of human surfactant protein A (SP-A) and SP-A variants. Am J Physiol Lung Cell Mol Physiol. 2008;294(1):L121-30.

163. Sibille Y, Reynolds HY. Macrophages and polymorphonuclear neutrophils in lung defense and injury. Am Rev Respir Dis. 1990;141(2):471-501.

164. Reynolds HY. Respiratory infections may reflect deficiencies in host defense mechanisms. Disease-a-month : DM. 1985;31(2):1-98.

165. Beilman G. Pathogenesis of oleic acid-induced lung injury in the rat: distribution of oleic acid during injury and early endothelial cell changes. Lipids. 1995;30(9):817-23.

166. Matute-Bello G, Frevert CW, Martin TR. Animal models of acute lung injury. Am J Physiol Lung Cell Mol Physiol. 2008;295(3):L379-99.

167. Dodd CE, Pyle CJ, Glowinski R, Rajaram MVS, Schlesinger LS. CD36-Mediated Uptake of Surfactant Lipids by Human Macrophages Promotes Intracellular Growth of Mycobacterium tuberculosis. The Journal of Immunology. 2016;197(12):4727-35.

168. Stewart CR, Stuart LM, Wilkinson K, van Gils JM, Deng J, Halle A, et al. CD36 ligands promote sterile inflammation through assembly of a Toll-like receptor 4 and 6 heterodimer. Nat Immunol. 2010;11(2):155-61.

169. Feinberg H, Taylor ME, Weis WI. Scavenger Receptor C-type Lectin Binds to the Leukocyte Cell Surface Glycan Lewisx by a Novel Mechanism. Journal of Biological Chemistry. 2007;282(23):17250-8.

170. Nakamura K, Funakoshi H, Miyamoto K, Tokunaga F, Nakamura T. Molecular cloning and functional characterization of a human scavenger receptor with C-type lectin (SRCL), a novel member of a scavenger receptor family. Biochemical and biophysical research communications. 2001;280(4):1028-35.

171. Cambi A, Figdor CG. Dual function of C-type lectin-like receptors in the immune system. Current opinion in cell biology. 2003;15(5):539-46.

172. Harris RJ, Elder D. Actin and Flagellin May Have an N-Terminal Relationship. Journal of Molecular Evolution. 2002;54(2):283-4.

173. Hatai H, Lepelley A, Zeng W, Hayden MS, Ghosh S. Toll-Like Receptor 11 (TLR11) Interacts with Flagellin and Profilin through Disparate Mechanisms. PLoS One. 2016;11(2):e0148987.

174. Salazar Gonzalez RM, Shehata H, O'Connell MJ, Yang Y, Moreno-Fernandez ME, Chougnet CA, et al. Toxoplasma gondii-Derived Profilin Triggers Human Toll-Like Receptor 5-Dependent Cytokine Production. Journal of innate immunity. 2014;6(5):685-94.

175. Hussell T, Bell TJ. Alveolar macrophages: plasticity in a tissue-specific context. Nat Rev Immunol. 2014;14(2):81-93.

176. Pollard TD. A Guide to Simple and Informative Binding Assays. Molecular Biology of the Cell. 2010;21(23):4061-7.

177. Hamilton RF, Jr., Thakur SA, Mayfair JK, Holian A. MARCO mediates silica uptake and toxicity in alveolar macrophages from C57BL/6 mice. The Journal of biological chemistry. 2006;281(45):34218-26.